

Synthesis and Some Reactions of the Heterometallic C₇ Complex $\{\text{Cp}^*(\text{dppe})\text{Ru}\}\text{C}\equiv\text{CC}\equiv\text{CC}\equiv\text{CC}\{\text{Co}_3(\mu\text{-dppm})(\text{CO})_7\}$

Michael I. Bruce,^{*,†} Marcus L. Cole,[†] Christian R. Parker,[†] Brian W. Skelton,[‡] and Allan H. White[‡]

School of Chemistry and Physics, University of Adelaide, Adelaide, South Australia 5005, and Chemistry M313, SBBCS, University of Western Australia, Crawley, Western Australia 6009

Received October 30, 2007

The heterometallic carbon-chain complex $\{\text{Cp}^*(\text{dppe})\text{Ru}\}\text{C}\equiv\text{CC}\equiv\text{CC}\equiv\text{CC}\{\text{Co}_3(\mu\text{-dppm})(\text{CO})_7\}$ (**1**) has been obtained by three routes that involve assembly of the C₇ chain by combination of appropriate C₁ + C₆, C₂ + C₅, or C₃ + C₄ precursors. The Cp analogue **2** and Co₃(CO)₉ cluster analogue **3** were obtained via the C₂ + C₅ and C₁ + C₆ routes, respectively. Reaction of **1** with PPh₃ gave **4** via substitution of a Co₃ cluster-bonded CO group. Addition of MeOTf to the second carbon from the Ru center in **1** afforded the vinylidene $[\{\text{Cp}^*(\text{dppe})\text{Ru}\}=\text{C}=\text{CMeC}\equiv\text{CC}\equiv\text{CC}\{\text{Co}_3(\mu\text{-dppm})(\text{CO})_7\}]\text{OTf}$ (**5**), while addition of tcne or tcnq across the central C≡C bond gave $\{\text{Cp}^*(\text{dppe})\text{Ru}\}\text{C}\equiv\text{CC}[\text{C}(\text{CN})_2]\text{C}[\text{C}(\text{CN})_2]\text{C}\equiv\text{CC}\{\text{Co}_3(\mu\text{-dppm})(\text{CO})_7\}$ (**6**) and $\{\text{Cp}^*(\text{dppe})\text{Ru}\}\text{C}\equiv\text{CC}[\text{C}_6\text{H}_4\text{C}(\text{CN})_2]\text{C}[\text{C}(\text{CN})_2]\text{C}\equiv\text{CC}\{\text{Co}_3(\mu\text{-dppm})(\text{CO})_7\}$ (**7**), respectively. The reaction between **1** and Fe₂(CO)₉ was more complex, the major product being $\{\text{Cp}^*(\text{dppe})\text{Ru}\}\text{C}\equiv\text{CC}\{\text{Fe}_3(\text{CO})_9\}\text{CC}\equiv\text{CC}\{\text{Co}_3(\mu\text{-dppm})(\text{CO})_7\}$ (**8**), accompanied by an Fe₂(CO)₆ derivative (**9**) of as yet undetermined structure. $\{\text{Cp}^*(\text{dppe})\text{Ru}\}\text{C}\equiv\text{CC}\equiv\text{CC}\equiv\text{CC}\{\text{Co}_2\text{Ni}(\mu\text{-dppm})(\text{CO})_4\text{Cp}\}$ (**10**) was obtained from the reaction with NiCp₂. An unstable adduct containing two Co₂(CO)₆ groups attached to the C₇ chain was formed in reactions between **1** and Co₂(CO)₈. XRD structural studies of **1**, **2**, **6–8**, and **10** are reported. Electrochemical measurements suggest that there is some interaction between the two end groups, although this cannot presently be quantified. It is concluded that the C₇ chain is long enough for the properties of the individual end caps to be preserved, while steric inhibition from the phenyl groups of the dppe and dppm ligands directs addition to the central C≡C triple bond of the C₇ chain.

Introduction

Many complexes of the type $\{\text{L}_x\text{M}\}(\text{C}\equiv\text{C})_n\{\text{ML}_x\}$ ($n = 1–10$), containing unsaturated carbon chains end-capped by redox-active groups such as MnX(dmpe)₂ ($X = \text{I}, \text{C}\equiv\text{CSiR}_3^2$), Mn(dmpe)Cp^{Me},³ Re(NO)(PPh₃)Cp*,⁴ Fe(CO)₂Cp*,⁵ Fe(PP)Cp* (PP = dppe, dippe),⁶ Ru(PP)Cp' [PP = (PPh₃)(PR₃), R = Me, Ph; dppm, dppe; Cp' = Cp, Cp*],⁷ and PtAr(PR₃)₂⁸ have been

found to undergo several stepwise one-electron oxidations. Theoretical calculations reveal that the HOMOs of these complexes generally have both metal and carbon character, the relative amounts of which depend on the nature of the end groups and the length of the carbon chain. Consequently, oxidation of these species can involve removal of electrons from orbitals localized predominantly either on the carbon chain itself (as in the Mn complexes)¹ or at the metal centers (as for Fe)⁶ or from orbitals that are delocalized over all atoms of the M–(C≡C)_x–M bridge.^{4,7} Calculations at various levels of theory reveal that the HOMOs of these complexes and their cations, although delocalized over the M–C_{2x}–M backbone, are more metallic in character for examples containing first-row transition metals,⁹ whereas they possess greater carbon character in the examples featuring second- and third-row transition metals.¹⁰

A detailed study of the heterobimetallic complexes $\{\text{Cp}^*(\text{dppe})\text{Fe}\}\text{C}\equiv\text{CC}\equiv\text{C}\{\text{Ru}(\text{dppe})\text{Cp}^*\}$ and $\{\text{Cp}^*(\text{dppe})\text{Fe}\}\text{C}\equiv\text{C}$

* Corresponding author. Fax: +61 8 8303 4358. E-mail: michael.bruce@adelaide.edu.au.

[†] University of Adelaide.

[‡] University of Western Australia.

(1) (a) Kheradmandan, S.; Heinze, K.; Schmalke, H. W.; Berke, H. *Angew. Chem., Int. Ed.* **1999**, *38*, 2270. (b) Fernandez, F. J.; Blacque, O.; Alfonso, M.; Berke, H. *Chem. Commun.* **2001**, 1266. (c) Fernandez, F. J.; Venkatesan, K.; Blacque, O.; Alfonso, M.; Schmalke, H. W.; Berke, H. *Chem.–Eur. J.* **2003**, *9*, 6192.

(2) Venkatesan, K.; Fox, T.; Schmalke, H. W.; Berke, H. *Organometallics* **2005**, *24*, 2834.

(3) Kheradmandan, S.; Venkatesan, K.; Blacque, O.; Schmalke, H. W.; Berke, H. *Chem.–Eur. J.* **2004**, *10*, 4872.

(4) (a) Brady, M.; Weng, W.; Zhou, Y.; Seyler, J. W.; Amoroso, A. J.; Arif, A. M.; Böhm, M.; Frenking, G.; Gladysz, J. A. *J. Am. Chem. Soc.* **1997**, *119*, 775. (b) Dembinski, R.; Lis, T.; Szafert, S.; Mayne, C. L.; Bartik, T.; Gladysz, J. A. *J. Organomet. Chem.* **1999**, *578*, 229. (c) Dembinski, R.; Bartik, T.; Bartik, B.; Jaeger, M.; Gladysz, J. A. *J. Am. Chem. Soc.* **2000**, *122*, 810.

(5) Akita, M.; Chung, M. C.; Sakurai, A.; Sugimoto, S.; Terada, M.; Tanaka, M.; Moro-oka, Y. *Organometallics* **1997**, *16*, 4882.

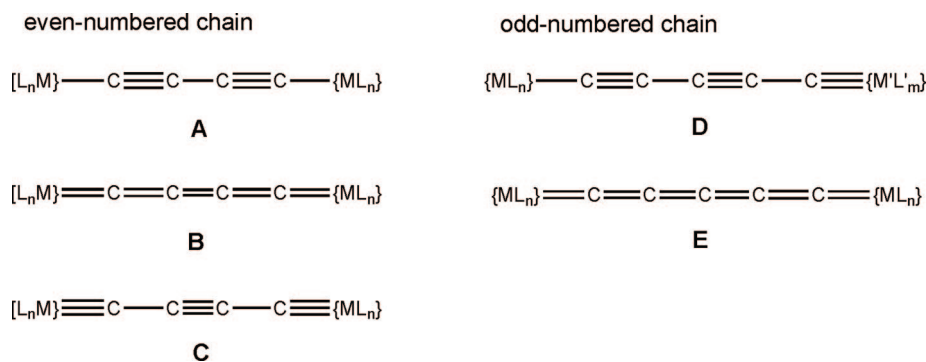
(6) (a) Le Narvor, N.; Toupet, L.; Lapinte, C. *J. Am. Chem. Soc.* **1995**, *117*, 7129. (b) Coat, F.; Lapinte, C. *Organometallics* **1996**, *15*, 477. (c) Coat, F.; GuilleVIC, M.-A.; Toupet, L.; Lapinte, C. *Organometallics* **1997**, *16*, 5988. (d) Le Narvor, N.; Lapinte, C. *C. R. Acad. Sci., Paris, Ser. IIC* **1998**, *1*, 745. (e) GuilleVIC, M.; Toupet, L.; Lapinte, C. *Organometallics* **1998**, *17*, 1928.

(7) (a) Bruce, M. I.; Low, P. J.; Costuas, K.; Halet, J.-F.; Best, S. P.; Heath, G. A. *J. Am. Chem. Soc.* **2000**, *122*, 1949. (b) Bruce, M. I.; Ellis, B. G.; Low, P. J.; Skelton, B. W.; White, A. H. *Organometallics* **2003**, *22*, 3184.

(8) (a) de Quadras, L.; Hampel, F.; Gladysz, J. A. *Dalton Trans.* **2006**, 2929. (b) Peters, T. B.; Bohling, J. C.; Arif, A. M.; Gladysz, J. A. *Organometallics* **1999**, *18*, 3261. (c) Zheng, Q.; Gladysz, J. A. *J. Am. Chem. Soc.* **2005**, *127*, 10508. (d) Owen, G. R.; Stahl, J.; Hampel, F.; Gladysz, J. A. *Organometallics* **2004**, *23*, 5889. (e) Owen, G. R.; Hampel, F.; Gladysz, J. A. *Organometallics* **2004**, *23*, 5893. (f) Zheng, Q.; Hampel, F.; Gladysz, J. A. *Organometallics* **2004**, *23*, 5896. (g) Mohr, W.; Stahl, J.; Hampel, F.; Gladysz, J. A. *Inorg. Chem.* **2001**, *40*, 3263.

(9) Paul, F.; Meyer, W. E.; Toupet, L.; Jiao, H.; Gladysz, J. A.; Lapinte, C. *J. Am. Chem. Soc.* **2000**, *122*, 9405.

Chart 1



$C\equiv C\{Ru(PPh_3)_2Cp\}$, which undergo stepwise oxidation with $[FeCp_2]PF_6$ to give the mono- and dications, $[\{Cp^*(dppe)Fe\}C\equiv C-C\equiv C\{Ru(dppe)Cp^*\}](PF_6)_n$, and $[\{Cp^*(dppe)Fe\}C\equiv CC\equiv C-\{Ru(PPh_3)_2Cp\}](PF_6)_n$ ($n = 1, 2$) has been reported.¹⁰ The available X-ray structural data, together with the IR spectrum of $[\{Cp^*(dppe)Fe\}C\equiv CC\equiv C\{Ru(PPh_3)_2Cp\}](PF_6)_2$, which shows a decrease in the $\nu(CC)$ frequency, are consistent with the gradual evolution of the polycarbon moiety from a diyndiyl structure (**A**, Chart 1) to a more cumulenic system (**B** or **C**) as oxidation proceeds. Computational studies indicate that there is a significant contribution from the iron center to the highest lying orbitals of the delocalized electronic structure. Spectroscopic results (⁵⁷Fe Mössbauer, ESR, IR, UV-vis, and NIR) support these conclusions, although detailed analysis of the NIR region, which is complicated by the overlapping of several other transitions with the lowest energy band, suggests that the major transition probably arises from photoinduced transfer of an electron from iron to ruthenium. These data allow an estimation of the relative contributions of the metal centers and ancillary ligands to the properties of the $[\{M\}-CC-CC-\{M'\}]^{n+}$ assemblies and clearly indicate the dominant role of ruthenium over iron in dictating the underlying electronic structures of C₄-bridged heterometallic complexes.¹⁰

Consequently, the behavior of other complexes containing dissimilar metal–ligand groups linked by unsaturated carbon chains has evoked interest. There is a relatively small number of complexes containing carbon chains linking two metal–ligand groups either from different periodic groups or with differing ligand environments. Detailed studies of $\{Cp^*(dppe)Fe\}C\equiv C-C_6H_4C\equiv C\{Re(CO)_3(bpy)\}$ have been reported,¹¹ one of the more interesting features being the quenching of luminescence associated with the rhenium center by addition of the iron group, which is restored upon oxidation to the 1⁺ cation.

Note that in complexes containing an odd-numbered carbon chain, those with poly-yne formulations have both σ -bonded and multiply bonded carbynic end groups (**D**), whereas the cumulenic forms may have two identical groups (**E**).

Several complexes containing a metal cluster acting as one of the end caps to a carbon chain have been isolated, in which the chain is attached via a μ - or μ_3 - η^1 -C atom or via a μ_3 - η^1, η^2 -C₂ unit.¹² Examples include $Ru_3\{\mu_3-CC\equiv[Mo(CO)_2Cp]\}(\mu-$

$CO)_3Cp'_3$ ($Cp' = Cp, Cp^{Me}$),¹³ $\{Os_3(\mu-H)\{\mu_3-C_2(C\equiv C)_x-$
 $[Re(NO)(PPh_3)Cp^*]\}(CO)_9$ ($x = 1, 2$),¹⁴ $[Cu_3(\mu-dppm)_3\{\mu_3-$
 $C\equiv CC\equiv C[Re(Me_2bpy)(CO)_3]\}_2]^+$,¹⁵ $Fe_2Ir\{\mu_3-\eta^1, \eta^2-C_2C\equiv C-$
 $[W(CO)_3Cp]\}(CO)_7(PPh_3)$,¹⁶ and $Ru_3\{\mu_3-\eta^1, \eta^2-CC\equiv CC-$
 $[Fe_2(\mu-CO)(CO)_2Cp^*]\}(\mu_3-CO)(CO)_9$.¹⁷ From studies designed to prepare related complexes containing odd-numbered carbon chains, we have described the compounds $\{(OC)_7(\mu-dppm)-$
 $Co_3\}\{\mu_3-C(C\equiv C)_x[ML_n]\}$ [e.g., $x = 1, 2, ML_n = W(CO)_3Cp,$
 $Au(PR_3)$ ($R = Ph, tol$), $Ru(dppe)Cp^*$, Fc, Fc'],¹⁸ although no detailed studies of their properties and reactivity have yet been reported.

This paper describes the synthesis and some chemistry of the complex $\{(OC)_7(\mu-dppm)Co_3\}C(C\equiv C)_3\{Ru(dppe)Cp^*\}$ (**1**), chosen because a C₇ chain is long enough to avoid steric hindrance by the phenyl groups of either of the diphosphine ligands, but short enough to allow some electronic interaction between the two end caps. In the course of examining the chemistry associated with this compound, we have demonstrated reactions of (a) the ruthenium center, (b) the tricobalt cluster, and (c) the carbon chain.

Results and Discussion

The construction of complexes containing two different end groups linked by carbon chains can be achieved by several routes, of which coupling of a terminal metalla-alkyne $\{ML_n\}(C\equiv C)_xCH$ (or precursor thereof) to the second metal center is perhaps the most convenient.^{19–22} An alternative approach consists of the coupling of two shorter carbon chains, for which we have recently developed an efficient route

(13) Griffith, C. S.; Koutsantonis, G. A.; Skelton, B. W.; White, A. H. *J. Organomet. Chem.* **2003**, 672, 17.

(14) Falloon, S. B.; Szafert, S.; Arif, A. F.; Gladysz, J. A. *Chem.–Eur. J.* **1998**, 4, 1033.

(15) Yam, V. W.-W.; Lo, W.-Y.; Lam, C.-H.; Fung, K.-M.; Wong, K. M.-C.; Lau, V. C.-Y.; Zhu, N. *Coord. Chem. Rev.* **2003**, 245, 39.

(16) Bruce, M. I.; Ellis, B. G.; Skelton, B. W.; White, A. H. *J. Organomet. Chem.* **2000**, 607, 137.

(17) Akita, M.; Chung, M.-C.; Sakurai, A.; Moro-oka, Y. *Chem. Commun.* **2000**, 1285.

(18) (a) Bruce, M. I.; Kramarczuk, K. A.; Zaitseva, N. N.; Skelton, B. W.; White, A. H. *J. Organomet. Chem.* **2005**, 690, 1549. (b) Antonova, A. B.; Bruce, M. I.; Humphrey, P. A.; Gaudio, M.; Nicholson, B. K.; Scoleri, N.; Skelton, B. W.; White, A. H.; Zaitseva, N. N. *J. Organomet. Chem.* **2006**, 691, 4694. (c) Bruce, M. I.; Skelton, B. W.; White, A. H.; Zaitseva, N. N. *J. Organomet. Chem.* **2003**, 683, 398.

(19) Weng, W.; Bartik, T.; Brady, M.; Bartik, B.; Ramsden, J. A.; Arif, A. M.; Gladysz, J. A. *J. Am. Chem. Soc.* **1995**, 117, 11922.

(20) Bruce, M. I.; Ke, M.; Low, P. J. *Chem. Commun.* **1996**, 21, 2405.

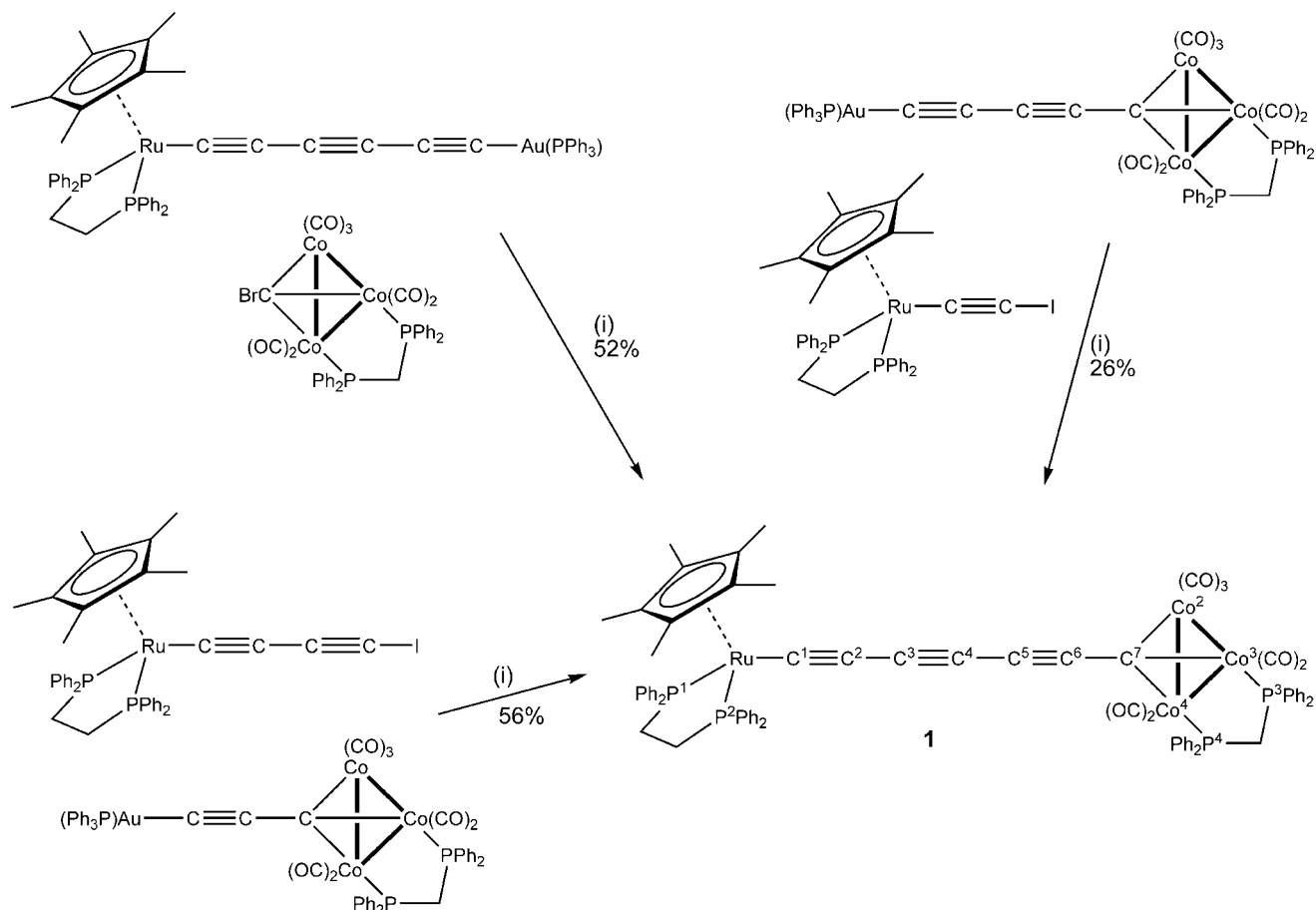
(21) Akita, M.; Chung, M.-C.; Sakurai, A.; Sugimoto, S.; Terada, M.; Tanaka, M.; Moro-oka, Y. *Organometallics* **1997**, 16, 4882.

(22) Pilar Gamasa, M.; Gimeno, J.; Godefroy, I.; Lastra, E.; Martín-Vaca, B. M.; García-Granda, S.; Gutierrez-Rodriguez, A. *J. Chem. Soc., Dalton Trans.* **1995**, 1901.

(10) Bruce, M. I.; Costuas, K.; Davin, T.; Ellis, B. G.; Halet, J.-F.; Lapinte, C.; Low, P. J.; Smith, M. E.; Skelton, B. W.; Toupet, L.; White, A. H. *Organometallics* **2005**, 24, 3864.

(11) Wong, K. M.-C.; Lam, S. C.-F.; Ko, C.-C.; Zhu, N.; Yam, V. W.-W.; Roué, S.; Lapinte, C.; Fathallah, S.; Costuas, K.; Kahlal, S.; Halet, J.-F. *Inorg. Chem.* **2003**, 42, 7086.

(12) For a recent review, see: Bruce, M. I.; Low, P. J. *Adv. Organomet. Chem.* **2004**, 50, 179.

Scheme 1^a

^a Reagent: (i) Pd(PPh₃)₄/CuI, thf.

involving elimination of phosphine-gold(I) halides from appropriate precursors.²³ In seeking to make the target molecule **1** discussed above, we have employed several variants of these reactions in order to achieve assembly of the C₇ chain via C_m + C_n → C₇ routes. Three approaches to the coupling of two shorter carbon chains were explored (Scheme 1). Novel intermediates were prepared by the Pd(0)/Cu(I)-catalyzed reactions between Ru{C≡CC≡CAu(PPh₃)}(dppe)Cp* and Me₃SiC≡Cl to give Ru{(C≡C)₃SiMe₃}(dppe)Cp* (83%), followed by treatment of the latter with AuCl(PPh₃) in the presence of NaOMe to give Ru{(C≡C)₃Au(PPh₃)}(dppe)Cp* (94%).

The reaction of Co₃{μ₃-CBr}(μ-dppm)(CO)₇ with Ru{(C≡C)₃Au(PPh₃)}(dppe)Cp*, resulting in the coupling C₁ + C₆ → C₇, afforded **1** in 52% yield. To link C₂ + C₅ → C₇, the complex Co₃{μ₃-C(C≡C)₂Au(PPh₃)}(μ-dppm)(CO)₇ was reacted with putative Ru(C≡Cl)(dppe)Cp*, prepared *in situ* by deprotonation of the vinylidene [Ru(=C=CH₂)(dppe)Cp*]⁺ with 2 equiv of LiBu, followed by addition of [I(py)₂]BF₄; this reaction afforded **1** in 26% yield. Although we have not yet succeeded in isolating the supposed intermediate iodoalkynyl complex Ru(C≡Cl)(dppe)Cp* in a pure state, Gamasa and co-workers have reported a similar reaction between Ru(C≡Cl)-(PPh₃)₂(η⁵-C₉H₇) and [I(py)₂]BF₄ to afford unstable Ru(C≡Cl)-(PPh₃)₂(η⁵-C₉H₇).²² A similar approach to coupling C₃ + C₄

→ C₇ chains was achieved by reacting Co₃{μ₃-CC≡CAu(PPh₃)}(μ-dppm)(CO)₇ with Ru(C≡CC≡Cl)(dppe)Cp*,²⁴ again prepared *in situ* from Ru(C≡CC≡CH)(dppe)Cp*, LiBu, and [I(py)₂]BF₄, to give **1** in 57% yield. In the ES-MS, obtained from solutions in MeOH containing NaOMe, ions at *m/z* 1499 ([M + Na]⁺), 1476 (M⁺), and 1448 ([M - CO]⁺) are present.

The Cp analogue of **1** was obtained from the reaction between the supposed Ru(C≡Cl)(dppe)Cp, prepared as the Cp* analogue above, and Co₃{μ₃-CC≡CAu(PPh₃)}(μ-dppm)(CO)₇, to give the dark brown complex {Cp(dppe)Ru}C≡CC≡CC≡CC{Co₃(μ-dppm)(CO)₇} (**2**) in 26% yield. The ES-MS, obtained from solutions in MeOH containing NaOMe, contains ions at *m/z* 1429 ([M + Na]⁺) and 1406 (M⁺).

A reaction between Co₃{μ₃-CBr}(CO)₉ and Ru{(C≡C)₃Au(PPh₃)}(dppe)Cp* gave {Cp*(dppe)Ru}C≡C-C≡CC≡CC{Co₃(CO)₉} (**3**) in 48% yield. This maroon compound is considerably less stable than either **1** or **2**. The negative-ion ES-MS contains [M + OMe]⁻ at *m/z* 1179.

Characterization of these complexes and the others described below has been achieved by microanalysis and spectroscopically, as well as by a single-crystal XRD study in some cases (see below). Spectroscopic data are summarized in Table 1. The IR and NMR spectra contain the expected absorptions; we defer until later a discussion of the resonances of the carbon chains in **1** and other complexes reported herein. The ³¹P NMR spectrum contains two equal-intensity signals at δ 33.9 and 80.2 from the dppm and dppe ligands, respectively.

(23) (a) Bruce, M. I.; Smith, M. E.; Zaitseva, N. N.; Skelton, B. W.; White, A. H. *J. Organomet. Chem.* **2003**, 670, 170. (b) Antonova, A. B.; Bruce, M. I.; Ellis, B. G.; Gaudio, M.; Humphrey, P. A.; Jevric, M.; Melino, G.; Nicholson, B. K.; Perkins, G. J.; Skelton, B. W.; Stapleton, B.; White, A. H.; Zaitseva, N. N. *Chem. Commun.* **2004**, 960.

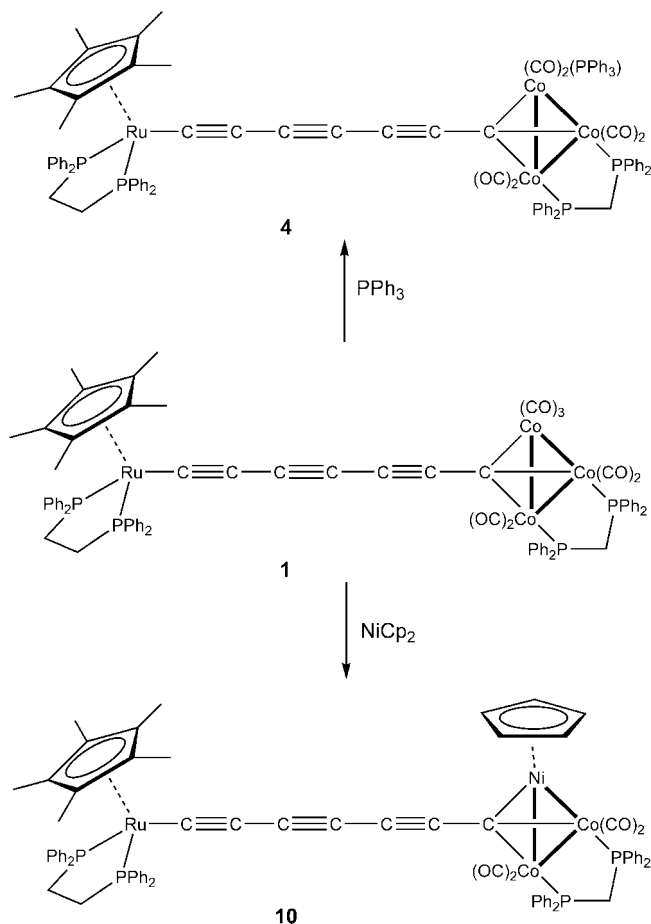
(24) Bruce, M. I.; Jevric, M.; Parker, C. R. Unpublished results.

Table 1. ¹³C NMR Chemical Shifts for Carbon Chains

complex ^a	#	C(1)	C(2)	C(4)	C(3)	C(5)	C(6)	C(7)	reference
[Ru]-C ₆ -SiMe ₃		137.58t	94.07	49.43	69.79	77.93	92.19		this work
[Ru]-C ₆ -Au(PPh ₃)		154.43	92.01/94.15	48.99	51.19	64.41	94.15/92.01		this work
[[Ru*]-CCMe-C ₅ -[Co ₃]]OTf	5	357.39t	109.04/107.56	97.32, 81.51, 91.04			107.56/109.04	215.09	this work
[Ru*]-C ₇ -[Co ₃]	1	151.88	94.88	48.79	90.70, 91.49		104.01		this work
[Ru*]-C ₇ -[Co ₂ Ni]	10	151.78	93.27	51.50	91.85, 92.33		107.50		this work
[Ru*]-C ₂ (C ₂ -tcne)C ₃ -[Co ₃]	6	151.03	105.56		75.43	83.65		216.58	this work
[Ru*]-C ₂ (C ₂ -tcnq)C ₃ -[Co ₃]	7	154.39/155.33	108.56		63.24	82.70			this work
[Ru*]-C ₂ C[Fe ₃]CC ₂ C-[Co ₃]	8	154.78	92.90	252.61, 273.10		80.50	114.09		this work
Me ₃ Si-C ₃ -[Co ₃]		126.19	116.70						18b
Fc-C ₃ -[Co ₃]		111.77	107.95						18b
Fc-C ₇ -[Co ₃]		99.03	97.13	63.38, 65.66, 72.73			80.95		18b
[Pt]-C ₄ -H			92.4	72.3	58.9				8

^a [Ru] = Ru(dppe)Cp; [Ru*] = Ru(dppe)Cp*; [Co₃] = Co₃(μ-dppm)(CO)₇; [Co₂Ni] = Co₂Ni(μ-dppm)(CO)₄Cp; [Fe₃] = Fe₃(CO)₉; [Pt] = *trans*-Pt(C₆F₅)(PAr₃)₂.

Scheme 2



Reactions of 1. It was of interest to examine the chemistry of **1** to determine how far the characteristic reactions of one end group are modified by the presence of the other. To this end, we have investigated reactions between **1** and PPh₃ [substitution of a Co(CO)₃ carbonyl group], methyl triflate [addition to C(2) to give a vinylidene complex], tetracyanoethene (tcne), 7,7,8,8-tetracyanoquinodimethane (tcnq), Co₂(CO)₈ and Fe₂(CO)₉ (which are expected to add to a C≡C triple bond in the C₇ chain), and NiCp₂ [either addition to a C≡C triple bond or replacement of the Co(CO)₃ group]. This chemistry is summarized in Schemes 2–4.

(a) With PPh₃. The ready substitution of one of the CO groups on the Co₃ cluster by PPh₃ was discovered serendipitously during a reaction with AuI(PPh₃). The thermal reaction between **1** and PPh₃ in refluxing thf afforded {Cp*(dppe)Ru}C≡C-

C≡C≡CC{Co₃(μ-dppm)(CO)₆(PPh₃)} (**4**) in 84% yield, surprisingly considerably better than that obtained from a similar reaction carried out in the presence of Me₃NO, which is often used to activate cluster-bound CO groups toward substitution (41%). The ³¹P NMR spectrum contains three resonances with 2:1:2 ratio, at δ 33.6 (d, dpmm), 48.4 (broad t, PPh₃), and 80.5 (s, dppe), confirming the site of PPh₃ substitution to be the third cobalt center. The ES-MS of solutions in MeOH containing NaOMe contained [M + Na]⁺ at *m/z* 1733.

(b) With MeOTf. A characteristic reaction of alkynyl-ruthenium complexes is the addition of electrophiles to C_β to give vinylidene complexes.²⁵ Addition of MeOTf to **1** at -78 °C, followed by warming to ambient temperature, resulted in a slow reaction (over 5 days) to give [{Cp*(dppe)Ru}C=CMe-C≡C≡CC{Co₃(μ-dppm)(CO)₇}]OTf (**5**), isolated in 63% yield as a brown solid. The slow rate of reaction is a surprise and not readily explained, since addition of electrophiles to alkynyl-ruthenium complexes is typically very fast. The presence of the alkynyl-vinylidene ligand is indicated by the characteristic downfield triplet at δ 357.39 [*J*(CP) = 16 Hz] in the ¹³C NMR spectrum assigned to Ru=C, together with the Me resonance at δ 10.15. The ³¹P NMR spectrum contains equal-intensity singlets at δ 34.9 (dpmm) and 74.0 (dppe). In the ES-MS, ions at *m/z* 1491 (M⁺) and 663 ([Ru(CO)(dppe)Cp*]⁺) are found.

(c) With tetracyanoethene (tcne) and 7,7,8,8-tetracyano-1,4-quinodimethane (tcnq). Reactions of tcne and tcnq with transition metal substrates generally result in the formation of charge transfer complexes or in oxidation reactions.²⁶ These properties result from the presence of low-lying π* orbitals in the cyanocarbons. The products are often radical ions or dianions, with concomitant formation of either side-on coordination, ion pairs, or nitrile-bonded complexes, such as the recently described [{Re(CO)₃(bpy)}₄(μ₄-tcnq)]⁴⁺ and [{Fe(CO)₂Cp}₄(tcnx)]⁴⁺ (tcnx = tcne, tcnq, tcnb), the formation of which involves very little charge transfer from metal to the cyanocarbon ligand.²⁷ The zwitterionic vinylidene complex Ru⁺{C=CPhCH(CN)(tcnq⁻)}(PPh₃)₂Cp was obtained from the reaction between tcnq and the cyclopropenyl complex Ru{C=CPhCH(CN)}(PPh₃)₂Cp.²⁸ More recently, Lapinte has

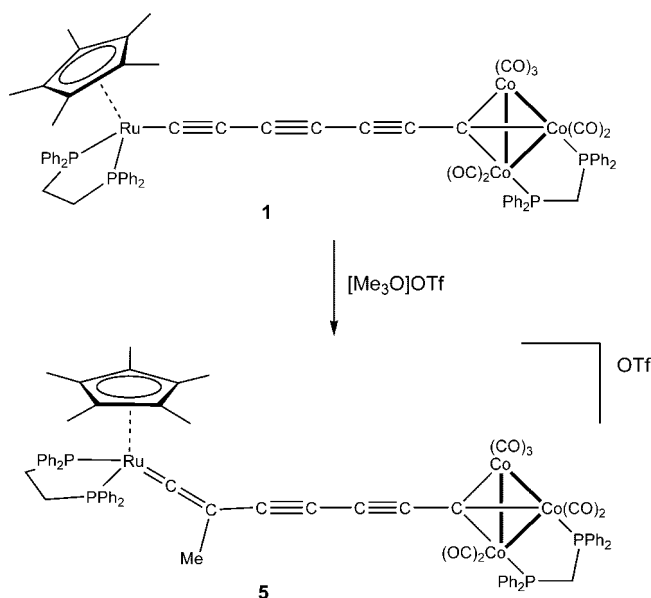
(25) (a) Bruce, M. I. *Chem. Rev.* **1991**, *91*, 197. (b) Bruce, M. I.; Swincer, A. G. *Adv. Organomet. Chem.* **1983**, *22*, 59.

(26) Kaim, W.; Moscherosch, M. *Coord. Chem. Rev.* **1994**, *129*, 157.

(27) (a) Hartmann, H.; Kaim, W.; Wanner, M.; Klein, A.; Franz, S.; Duboc-Toia, C.; Fiedler, J.; Zális, S. *Inorg. Chem.* **2003**, *42*, 7018. (b) Maity, A. N.; Schwederski, B.; Sarkar, B.; Zális, S.; Fiedler, J.; Kar, S.; Lahiri, G. K.; Duboc, C.; Grunert, M.; Gülich, P.; Kaim, W. *Inorg. Chem.* **2007**, *46*, 7312.

(28) Ting, P.-C.; Lin, Y.-C.; Lee, G.-H.; Cheng, M.-C.; Wang, Y. *J. Am. Chem. Soc.* **1996**, *118*, 6433.

Scheme 3



described the use of *tcnq* as an oxidizing agent, its reaction with 9,10- $[\text{Fe}(\text{dppe})\text{Cp}^*(\text{C}\equiv\text{C})]_2$ -anthracene affording the well-crystallized ion pair [9,10- $\{\text{Cp}^*(\text{dppe})\text{Fe}(\text{C}\equiv\text{C})\}_2\text{C}_{14}\text{H}_8$](*tcnq*).²⁹

In contrast, the reactions of *tcne* and several analogous cyanoalkenes with unsaturated hydrocarbyl systems, particularly unsaturated C(sp) chains, attached to electron-rich metal centers, result in initial formal [2 + 2]-cycloaddition of the cyano-alkene to a C₂ moiety. In the case of *tcne*, this gives a tetracyanocyclobutenyl group, the reaction often being followed by ring-opening to give tetracyanobutadienyl derivatives.^{30,31} In some cases, paramagnetic intermediates can be detected at the first stages of the reaction, suggesting the intermediacy of radical species. Similar chemistry of *tcnq* is rare, the only well-substantiated example being the reactions of *trans*-Pt(C≡CR)₂(PR'₃)₂ (R = H, Me; R' = Me, Et), which afforded stable, deep purple 1:1 adducts. Although initially formulated as charge transfer complexes,³² a single-crystal XRD structure determination of the Pt-propynyl adduct revealed that one C≡C triple bond had formally inserted into one of the =C(CN)₂ double bonds to give *trans*-Pt(C≡CMe) $\{C[=C_6H_4=C(CN)_2]CMe=C(CN)_2\}$ (PMe)₃.³³ Apparently only one isomer is formed, shown by the structural determination to be that in which the =C(CN)₂ group is attached to the outer carbon of the C≡CMe triple bond.

The reaction between **1** and *tcne* in dichloromethane proceeds rapidly through an initial dark purple coloration to black after 5 min. Workup gave black $\{\text{Cp}^*(\text{dppe})\text{Ru}\}C\equiv CC[=C(\text{CN})_2]C[=C(\text{CN})_2]C\equiv CC\{Co_3(\mu\text{-dppe})(CO)_7\}$ (**6**) in 86% yield, crystallographically identified (see below) as the product of formal insertion of the central C≡C triple bond into the C=C double bond of the alkene. The overall composition of **6** was confirmed by microanalysis and the ES-MS, which contains $[M + Na]^+$

and M⁺ ions at *m/z* 1627 and 1604, respectively. A band assigned to $\nu(\text{CN})$ (2210 cm⁻¹) present in the IR spectrum is more informative. Signals for the Cp*, CH₂, and Ph groups in the ¹³C NMR spectrum are accompanied by weaker singlets at δ 113.63, 113.90, 116.64, 116.83 (CN) and 201.82 (CO). The ³¹P NMR spectrum contains, in place of the usual singlets, two AB quartets centered at δ 34.9 [*J*(PP) = 47 Hz, dppm] and 80.1 [*J*(PP) = 10 Hz, dppe] arising from the nonequivalence of the two ³¹P nuclei in the respective chelating diphosphines, which in turn results from the marked asymmetry of the cyanocarbon bridge. Similar coupling of the ³¹P resonances of dppe ligands has been observed for the related complexes $\{(\text{CO})_7(\mu\text{-dppe})Co_3\}CC\equiv CC[=C(\text{CN})_2]C[=C(\text{CN})_2]C[Co_3(\mu\text{-dppe})(CO)_7]$ ^{23a} and $\text{Ru}\{C\equiv CC[=C(\text{CN})_2]CFC=C(\text{CN})_2\}(\text{dppe})\text{Cp}$,³⁴ which also contain unsymmetrically coordinated cyanocarbon ligands.

As found for *tcne*, the reaction between **1** and *tcnq* proceeds rapidly in dichloromethane, via several color changes, to give a dark blue solution, from which the complex $\{\text{Cp}^*(\text{dppe})\text{Ru}\}\{\mu\text{-C}\equiv CC[=C_6H_4=C(\text{CN})_2]C[=C(\text{CN})_2]C\equiv CC\}\{Co_3(\mu\text{-dppe})(CO)_7\}$ (**7**) was obtained in 86% yield. Correct microanalyses were obtained and supported by ions at *m/z* 1703 and 1680 for $[M + Na]^+$ and M⁺ in the ES-MS obtained from a solution containing NaOMe. The IR spectrum of a dichloromethane solution contained a $\nu(\text{CN})$ band at 2193 cm⁻¹ and medium-intensity bands at 1585 and 1369 cm⁻¹, which we assign to the =C₆H₄= moiety. The ¹H NMR spectrum contains two singlets at δ 6.18 and 6.21 (CH of C₆H₄) and aromatic protons between δ 6.63 and 7.71. In the ¹³C NMR spectrum, the expected signals for the Cp*, dppe, dppm, and aromatic carbons are accompanied by four singlets between δ 114 and 118 (CN) and a multiplet at δ 201.62 [Co-CO]. The ³¹P NMR spectrum exhibits broad resonances at δ 33.3 (dppm) and a broad doublet at 79.6 (dppe) [*J*(PP) = 369 Hz]. The molecular structure of **7** is discussed below.

(d) With Fe₂(CO)₉. We next examined the reactions of **1** with reactive metal complexes that might be expected to react with either of the end groups or with the C₇ chain. The reaction of **1** with Fe₂(CO)₉, which is known to exchange CO for PPh₃ in complexes $\text{RuX}(\text{PPh}_3)_2\text{Cp}$,³⁵ to replace Co(CO)₃ groups by FeH(CO)₃ in CO₃ clusters,^{36,37} or to cleave C≡C triple bonds in carbon chain complexes,^{38,39} afforded several products in small yield. Optimization of reaction conditions (see Experimental Section) afforded a major purple product, identified crystallographically as $\{\text{Cp}^*(\text{dppe})\text{Ru}\}C\equiv CC\{Fe_3(\text{CO})_9\}CC\equiv CC\{Co_3(\mu\text{-dppe})(CO)_7\}$ (**8**). The IR spectrum contains $\nu(\text{CO})$ bands between 2069 and 1913 cm⁻¹, although the $\nu(\text{C}\equiv\text{C})$ bands could not be positively identified. The ³¹P NMR spectrum contains the expected dppm and dppe resonances at δ 35.2 and 78.5, respectively. In the ES-MS, $[M + Na]^+$ and M⁺ occur at *m/z* 1918 and 1896, respectively.

Formation of **8** involves formal cleavage of possibly one of the strongest bonds in the molecule and results in C(3) and C(4) capping both sides of the Fe₃ triangle. This reaction has previously been observed with other poly-ynediyl molecules

(29) de Montigny, F.; Argouarch, G.; Costuas, K.; Halet, J.-F.; Roisnel, T.; Toupet, L.; Lapinte, C. *Organometallics* **2005**, *24*, 4558.

(30) Davison, A.; Solar, J. P. *J. Organomet. Chem.* **1979**, *166*, C13.

(31) (a) Bruce, M. I.; Hambley, T. W.; Snow, M. R.; Swincer, A. G. *Organometallics* **1985**, *4*, 494. (b) Bruce, M. I.; Hambley, T. W.; Snow, M. R.; Swincer, A. G. *Organometallics* **1985**, *4*, 501. (c) Bruce, M. I.; Low, P. J.; Skelton, B. W.; White, A. H. *New J. Chem.* **1998**, *22*, 419.

(32) Masai, H.; Sonogashira, K.; Hagihara, N. *J. Organomet. Chem.* **1972**, *34*, 397.

(33) Onuma, K.-I.; Kai, Y.; Yasuoka, N.; Kasai, N. *Bull. Chem. Soc. Jpn.* **1975**, *48*, 1696.

(34) Bruce, M. I.; de Montigny, F.; Jevric, M.; Lapinte, C.; Skelton, B. W.; Smith, M. E.; White, A. H. *J. Organomet. Chem.* **2004**, *689*, 2860.

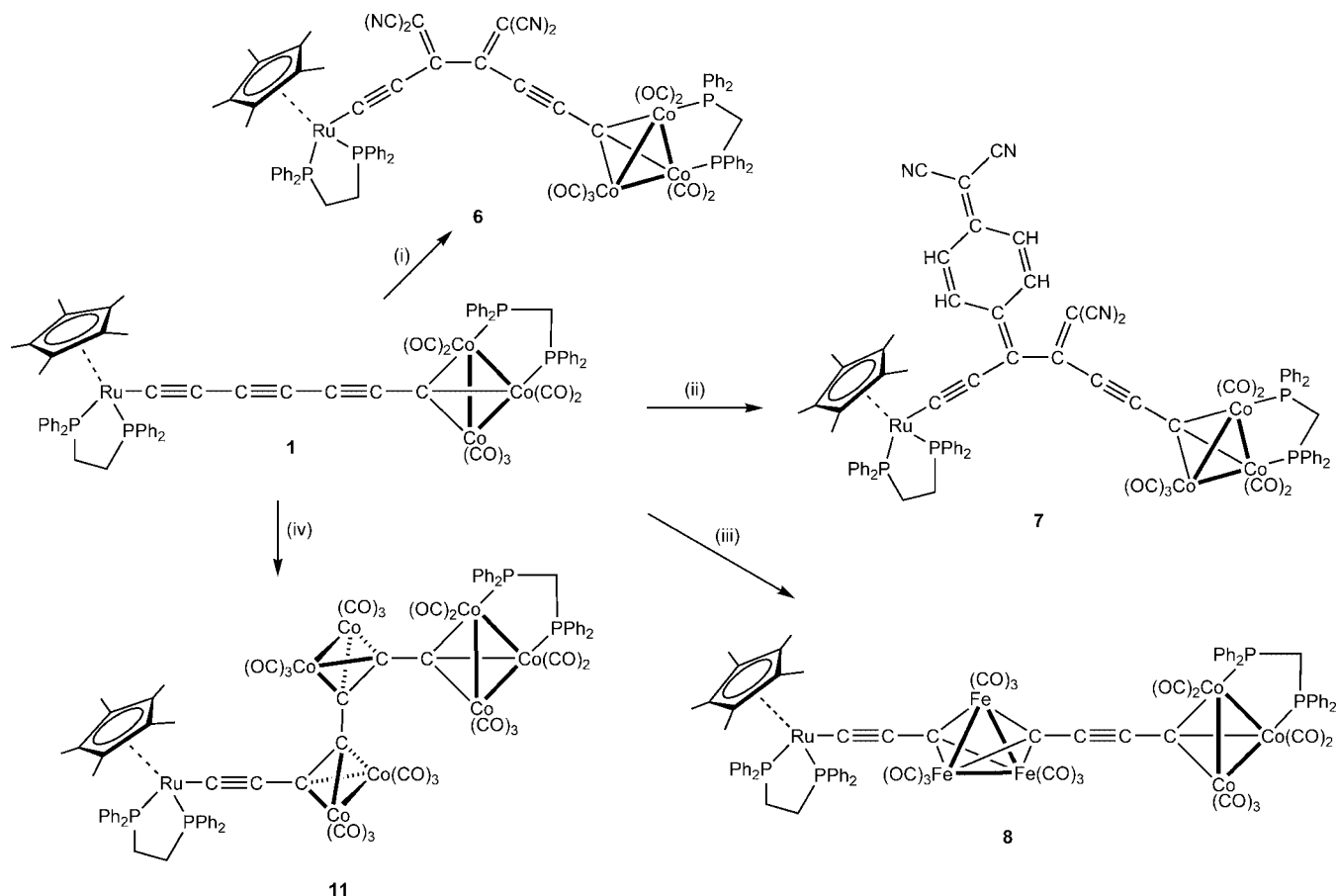
(35) Blackmore, T.; Bruce, M. I.; Stone, F. G. A. *J. Chem. Soc. A* **1971**, 2376.

(36) Blumhofer, R.; Vahrenkamp, H. *Chem. Ber.* **1986**, *119*, 683.

(37) Duffy, D. N.; Kassis, M. M.; Rae, A. D. *J. Organomet. Chem.* **1993**, *460*, 97.

(38) (a) Akita, M.; Sakurai, A.; Moro-oka, Y. *Chem. Commun.* **1999**, 101. (b) Akita, M.; Sakurai, A.; Chung, M.-C.; Moro-oka, Y. *J. Organomet. Chem.* **2003**, *670*, 2.

(39) Bruce, M. I.; Ellis, B. G. Unpublished results.

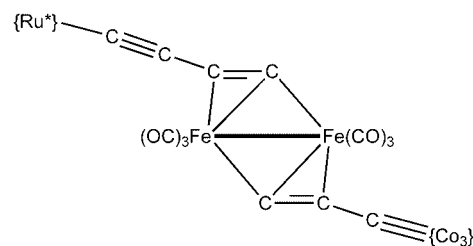
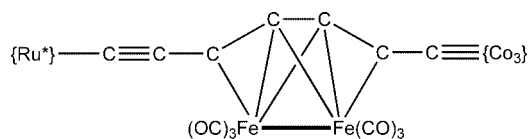
Scheme 4^a

^a Reagents: (i) tcne; (ii) tcnq; (iii) Fe₂(CO)₉; (iv) Co₂(CO)₈.

such as Fp*(C≡C)_xFp*³⁸ and {Ru(dppe)Cp*}(C≡C)_x{Ru(dppe)Cp*} (x = 3, 4),³⁹ and it has been suggested³⁸ that it proceeds via a pseudotetrahedral C₂Fe₂(CO)₆ intermediate, which then rapidly picks up a third Fe(CO)₃ fragment. In these cases, an even-numbered C_x chain is cleaved to form two odd-numbered carbon chains, while in the reaction with **1**, the C₇ chain forms C₃ + C₄ chains as a result of the formation of the bis-carbyne C₄ ligand, previously found in {Co₃(μ-dppm)_n(CO)_{9-2n}}₂(μ-C₄) (n = 0,⁴⁰ 1⁴¹) and {MCo₂(CO)₈Cp}₂(μ-C₄) (M = Mo, W, Mo/W)⁴² and postulated to be related to the structure **C** of the 4e-oxidized product from {Ru(PP)Cp'}₂(μ-C₄).⁷

While several other products are formed in varying amounts in the reactions between **1** and Fe₂(CO)₉, with one exception we have not succeeded in isolating them in pure form. A green-brown compound **9** has been isolated from reaction in thf and appears to be favored over **8** at elevated temperatures. Compound **9** is thought to be a Fe₂(CO)₆ adduct from its ES-MS, *m/z* 1779 and 1756 for [M + Na]⁺ and M⁺ obtained from a solution containing NaOMe. To date it has not been possible to obtain X-ray quality crystals of **9**. With only terminal ν(CO) bands in the IR spectrum, we may speculate that two central C≡C triple bonds have interacted with the Fe₂(CO)₉ reagent with displacement of three CO groups; that is, the carbon chain acts as a six-electron donor. Two structures

can be suggested, one involving coordination of the carbon chain in a manner reminiscent of the well-known “flyover” complexes (**F**), while the other contains two fragments formed by cleavage of a central C–C bond, the chain forming a μ-η¹,η² ligand to each of two Fe(CO)₃ groups (**G**). Although this complex does not appear to be an intermediate en route to **8**, cleavage of the carbon chain is an attractive formulation, based on the product ratio in reactions carried out at higher temperatures.



(40) Dellaca, R. J.; Penfold, B. R.; Robinson, B. H.; Robinson, W. T.; Spencer, J. L. *Inorg. Chem.* **1970**, *9*, 2204.

(41) Bruce, M. I.; Skelton, B. W.; White, A. H.; Zaitseva, N. N. *Organometallics* **2006**, *25*, 4817.

(42) Bruce, M. I.; Halet, J.-F.; Kahlal, S.; Low, P. J.; Skelton, B. W.; White, A. H. *J. Organomet. Chem.* **1999**, *578*, 155.

(e) With NiCp₂. Reactions of CCo₃ clusters with NiCp₂ or {Ni(μ-CO)Cp}₂ result in replacement of a Co(CO)₃ group

by NiCp.⁴³ The reaction between **1** and an equivalent amount of NiCp₂ was carried out in refluxing thf and afforded brown {Cp*(dppe)Ru}C≡CC≡CC≡CC{Co₂Ni(μ-dppm)(CO)₄Cp} (**10**) in 41% yield. This complex was characterized spectroscopically and by a single-crystal XRD study. Terminal +ν(CO) bands occur in the IR spectrum between 2076 and 1939 cm⁻¹, while in the ES-MS, M⁺ and [M + Na]⁺ are found at *m/z* 1456 and 1479, respectively. In the ¹H NMR spectrum, Resonances at δ_H 1.57 (RuCp*) and 5.44 (NiCp) and δ_C 10.52 and 94.50 (RuCp*) and 90.26 (NiCp) and two singlets at δ_P 23.6 (dppm) and 80.3 (dppe) support the structural assignment. In the ³¹P NMR spectrum, there is a considerable upfield shift of the dppm resonance to δ_P 23.6 resulting from replacement of the Co(CO)₃ group by NiCp.

(f) With Co₂(CO)₈. Attempted addition of a Co₂(CO)₆ fragment to the C₇ chain by reacting **1** with Co₂(CO)₈ gave a dark green-brown solid, which quickly reverted to **1** during chromatography on silica or alumina or on exposure of solutions to air. The product is tentatively identified as the bis-adduct {Cp*(dppe)Ru}{C≡CC₂[Co₂(CO)₆]₂C₂[Co₂(CO)₆]₂C{Co₃(μ-dppm)(CO)₇} (**11**). Identification of **11** rests largely on the ES-MS ([M + Na]⁺ at *m/z* 2071), as the NMR spectra are similar (but less well resolved) to those of **1** itself. The ³¹P NMR spectrum contains a doublet at δ 33.8 (dppm) [*J*(PP) = 24 Hz] and a singlet at δ 81.0 (dppe), suggesting that reaction occurred on C(3)≡C(4) and C(5)≡C(6). Although a mixture of **1** with Co₂(μ-dppm)(CO)₆ darkened on warming, the only isolable compounds proved to be **1** and Co₄(μ-dppm)₂(CO)₈.⁴⁴ It appears that the steric environment about the C₇ chain in **1** is too demanding to allow this dicobalt fragment to coordinate and form a stable complex.

General Comments. (a) ¹³C NMR Spectra of Carbon Chain Nuclei. Assignment of the resonances of the C₇ chain in **1** and other compounds described herein was made by comparison with the ¹³C NMR spectra of related compounds (Table 1). Resonances of the chain carbons in **2** were not found, due to poor solubility. The resonance of C(7) (numbering from Ru to Co₃, in accord with the crystallographic numbering schemes) was often not observed, because of the well-known broadening of this carbon by the ⁵⁹Co quadrupole.^{45,46} However, the spectra of the more soluble compounds **5** and **6** contain broad resonances at δ 215.1 and 216.6, respectively, which are assigned to C(7). In **8**, two of the three carbyne carbon resonances, assigned to the CFe₃ carbons, are found at δ 252.61 and 273.10.

A peak at δ ca. 150 is present in most compounds, but notably absent in the spectrum of the methylvinylidene adduct **5**, and is thus assigned to C(1) attached to the Ru center. In its place, the spectrum of **5** contains the characteristic downfield triplet at δ 357.39 [*J*(CP) = 16 Hz] assigned to Ru=C(1), together with the Me resonance at δ 10.15. In related alkynyl-Ru complexes, atom C(2) affords a resonance at δ ca. 92, and we assign resonances in this region similarly. The cationic center in vinylidene complexes results in a downfield shift to δ ca. 100, so that one of the two resonances in this region of the spectrum of **5** probably arises from C(2). For complexes Co₃(μ₃-

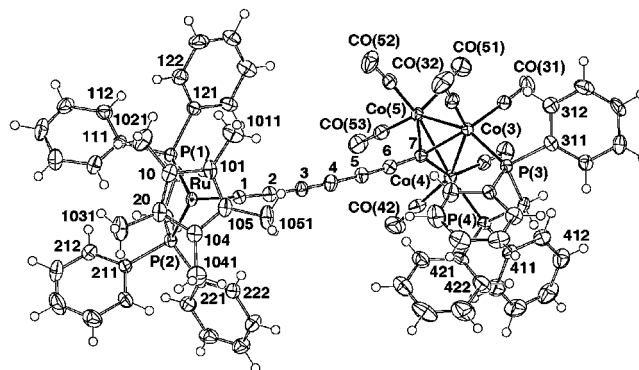


Figure 1. Projection of a molecule of {Cp*(dppe)Ru}(C≡C)₃C{Co₃(μ-dppm)(CO)₇} (**1**) in 1·2thf. [In this and later figures, the projections are normal to the Cp*(Ru) plane.]

CC≡CR)(μ-dppm)(CO)₇ (R = Bu^t, SiMe₃, Fc), the two alkynyl carbons resonate at δ 101.1, 116.7, 107.95 and 121.95, 126.2, 111.8, respectively, so that resonances listed here in the region δ 105–110 probably arise from C(6). The remaining resonances are not easily assigned: in longer carbon chains, the resonances of the central carbons tend toward δ ca. 60.⁴⁷ We note that in the present compounds resonances in this area are not found when the carbon chain has entered into reaction, destroying its poly-yne nature, as in **6–8**, so that in **1** and **10** we assign resonances at δ ca. 50 to C(3). It is expected that the C(5) resonance would be downfield from C(3) and resonances in **1** and **10** at δ ca. 90 are assigned to this atom. It has not been possible to assign the remaining resonances definitively to C(4, 5, 6).

(b) Molecular Structures. The molecular structures of **1**, **2**, **6–8**, and **10** (Figures 1–5) have been determined by XRD studies, selected bond distances and angles being collected in Table 2.

For **6**: C(3)–C(30) 1.378(9), C(4)–C(40) 1.376(10), C(30)–C(301, 302) 1.413, 1.427(9), C(40)–C(401, 402) 1.44, 1.42(1), C–N 1.141(9), 1.145(9), 1.136(12), 1.119(12) Å. C(2,4)–C(3)–C(30) 126.4(6), 117.5(6), C(3, 5)–C(4)–C(40) 119.3(7), 121.9(6), C(n01)–C(n0)–C(n02) 118.5(6), 118.3(7) (*n* = 3, 4)°.

For **7**: C(3)–C(301) 1.46(2), C(4)–C(8) 1.53(2), C(301)–C(302, 306) 1.37(2), 1.35(2), C(302)–C(303) 1.32(2), C(303)–C(304) 1.42(2), C(304)–C(300, 305) 1.42(2), 1.40(2), C(305)–C(306) 1.42(2) Å; C(2, 4)–C(3)–C(301) 125.7(1), 115.1(1), C(3, 5)–C(4)–C(8) 113.4(1), 118.8(1), C(304)–C(300)–C(307, 308) 123.0(1), 122.2(1), C(307)–C(300)–C(308) 114.1(1)°.

For **8** in 8·2C₆H₆: [Read Co(7,5,6) for Co(2,3,4)] Fe(2)–Fe(3, 4) 2.517(1), 2.545(1), Fe(3)–Fe(4) 2.528(1), C(3)–Fe(2, 3, 4) 2.011(5), 1.976(4), 2.010(5), C(4)–Fe(2, 3, 4) 1.944(4), 1.976(5), 1.949(5) Å. C(2)–C(3)–Fe(2, 3, 4) 133.8(3), 134.4(4), 131.0(4), C(5)–C(4)–Fe(2, 3, 4) 130.2(4), 131.6(4), 133.3(4)°.

For **8** in 8·CH₂Cl₂: [Read Co(7,5,6) for Co(2,3,4)] Fe(2)–Fe(3, 4) 2.5228(9), 2.5189(9), Fe(3)–Fe(4) 2.5265(10), C(3)–Fe(2, 3, 4) 2.003(4), 1.966(4), 1.986(4), C(4)–Fe(2, 3, 4) 1.952(4), 1.967(4), 1.944(4) Å. C(2)–C(3)–Fe(2, 3, 4) 133.9(3), 132.3(3), 132.1(3), C(5)–C(4)–Fe(2, 3, 4) 129.2(3), 130.2(3), 135.8(3)°.

For **10**: [For Co(2), read Ni(2)] Ni–C(cp) 2.093(9)–2.116(8), av 2.104(9) Å.

{Cp*(dppe)Ru}C≡CC≡CC≡CC{Co₃(μ-dppm)(CO)₇} (Cp* = Cp***1**, Cp**2**) and {Cp*(dppe)Ru}C≡CC≡CC≡CC{Co₂Ni(μ-dppm)(CO)₄Cp}, **10**. Two different solvates of **1**, which are

(43) (a) Beurich, H.; Blumhofer, R.; Vahrenkamp, H. *Chem. Ber.* **1982**, *115*, 2409. (b) Mlekuz, M.; Bougeard, P.; McGlinchey, M. J.; Jaouen, G. *J. Organomet. Chem.* **1983**, *253*, 117.

(44) Bruce, M. I.; Carty, A. J.; Ellis, B. G.; Low, P. J.; Skelton, B. W.; White, A. H.; Udachin, K. A.; Zaitseva, N. N. *Aust. J. Chem.* **2001**, *54*, 277.

(45) Aime, S.; Milone, L.; Valle, M. *Inorg. Chim. Acta* **1976**, *18*, 9.

(46) Yuan, P.; Richmond, M. G.; Schwarz, M. *Inorg. Chem.* **1990**, *29*, 679.

(47) Eisler, S.; Slepokov, A. D.; Elliott, E.; Luu, T.; McDonald, R.; Hegmann, F. A.; Tykwinski, R. R. *J. Am. Chem. Soc.* **2005**, *127*, 2666.

not isomorphous, were studied: following an initial determination on material crystallized from chloroform, yielding a result of unsatisfactory precision, a more auspicious result was obtained on crystals of a different solvate, obtained from thf. A projection of the molecule in the latter is shown in Figure 1. All compounds but **2** contain the Ru(dppe)Cp* fragment, which has the usual pseudo-octahedral geometry [Ru–P 2.260(2)–2.306(1), Ru–C(cp) 2.227(4)–2.326(14) Å, angles P(1)–Ru–P(2) 79.82(6)–85.0(1), P(1,2)–Ru–C(1) 76.8(2)–90.7(1)°]. In **1** and **2**, significant differences between the two P(1,2)–Ru–C(1) angles are found in the CHCl₃ solvate of **1** [84.7, 89.2(2)°] and **2** [84.9, 92.4(2)°], while in the thf solvate of **1**, these angles are close, at 84.6, 85.6(1)°. Similar differences have been found in most of the complexes containing Ru(PR₃)₂Cp* groups, but it is not clear whether they arise from a Jahn–Teller effect in the d⁶ center or from steric interactions within the crystal. The Ru–C(1) separations are experimentally indistinguishable.

At the other end of the carbon chain is the metal cluster, which is Co₃(μ-dppm)(CO)₇ for **1**, **2**, and **6–8** and Co₂Ni(μ-dppm)(CO)₄Cp for **10**. The geometries of the CO clusters are similar, the dppm ligand bridging the Co(3)–Co(4) vector. Bonds to Co are Co–Co 2.461(2)–2.4968(9), Co–P 2.188(2)–2.241(2) Å; the Co(1,2)–C(7) bonds are shorter [1.889(5)–1.93(1) Å] than Co(3)–C(7) [1.93(1)–1.977(4) Å], the latter showing the usual lengthening of this bond involving a Co(CO)₃ group. These values are similar to those found in numerous related structures.^{18,23a,48–52} In **10** (Figure 3), replacement of a Co(CO)₃ group by NiCp results in formation of two Ni–Co bonds [2.381(1), 2.397(1) Å], shorter separations reflecting the different radii of the two metal atoms. Similar differences are found in Co₂Ni(μ₃-CPh)(μ-PPh₂CH=CHPPh₂)(CO)₄Cp [Co–Co 2.464(1), Co–Ni 2.364(1), 2.385(1) Å]⁵³ and Co₂Ni(μ₃-CCO₂Me)(CO)₆Cp [Co–Co 2.471(2), Co–Ni 2.380(2) Å].⁵⁴ The Ni–C(cp) distances range between 2.093(9) and 2.116(8) Å [av 2.104(9) Å], and the Co₂Ni bonds to C(7) [Co(3,4)–C(7) 1.912(6), 1.895(6) Å; Ni(2)–C(7) 1.895(5) Å] are experimentally indistinguishable, as found in the similar diphosphine-substituted cluster mentioned above.⁵³

The C₇ chain is a point of interest in the molecules of **1**, **2**, and **10**. Separations between atoms C(1)–C(7) show that a –C≡C–C≡C–C≡C–C≡ system is present. There is an interesting alternation of the C≡C triple bonds [C(1)–C(2) 1.228(8)–1.241(6), C(3)–C(4) 1.21(1)–1.232(7), C(5)–C(6) 1.22(1)–1.226(7) Å], which is accompanied by a similar lengthening of the C(sp)–C(sp) single bonds [C(2)–C(3) 1.33(1)–1.350(8), C(4)–C(5) 1.350(7)–1.36(1), C(6)–C(7) 1.393(7)–1.40(1) Å], consistent with an alternation in effect of the filled Ru–C(1) π-type interaction along the C₇ chain from Ru to Co₃. To our knowledge, the molecular structure of HC≡CC≡CC≡CH does not appear to have been determined so far, probably because of its explosive character, but high-level [CCSD(T)/cc-pVTZ] computational studies have given values of 1.212, 1.365, and 1.217 Å for the CC separations

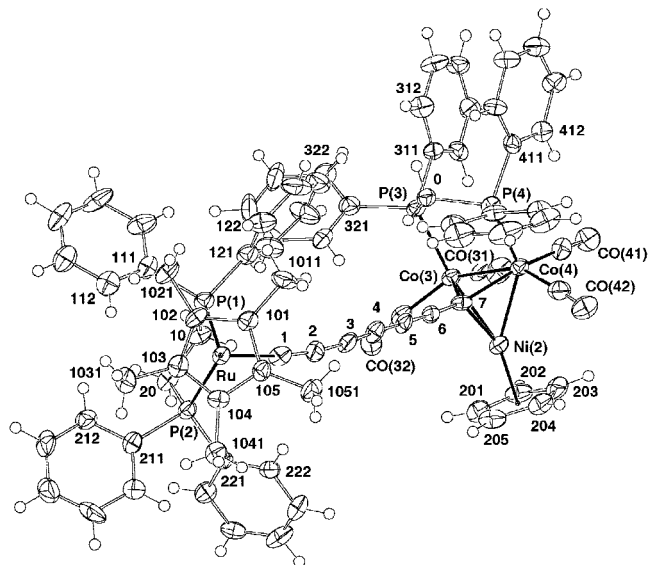


Figure 2. Projection of a molecule of {Cp*(dppe)Ru}(C≡C)₃-C{Co₂Ni(μ-dppm)(CO)₄Cp} (**10**) in 10·0.32C₆H₁₄.

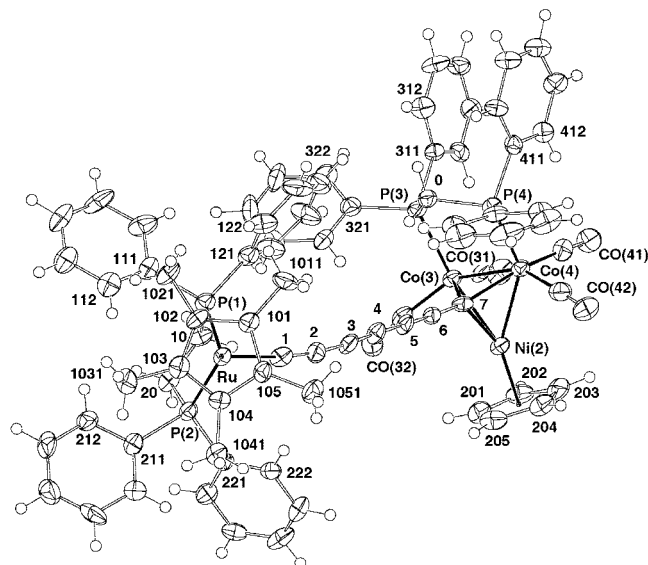


Figure 3. Projection of a molecule of {Cp*(dppe)Ru}C≡C{C[=C(CN)₂]}₂C≡CCo₃(μ-dppm)(CO)₇ (**6**) in 6·2Me₂CO.

(outermost–innermost).⁵⁵ Values for closely related compounds include 1.198, 1.377, 1.208 Å [for (HO)CH₂(C≡C)₃CH₂(OH)],⁵⁶ 1.169, 1.397, 1.184 Å [for {(Cy₃P)Au}(C≡C)₃{Au(PCy₃)}],⁵⁷ 1.210, 1.383, 1.213 Å [for {Cp(Ph₃P)₂Ru}(C≡C)₃{Ru(PPh₃)₂-Cp}]⁵⁸ and 1.226, 1.345, 1.221, 1.347 Å [for {(OC)₇(μ-dppm)Co₃}{μ₃-C(C≡C)₄-μ₃-C}{Co₃(μ-dppm)(CO)₇}]^{23a}. The respective lengthening and shortening of the C≡C triple and C–C single bonds suggest a degree of conjugation in the chain. As shown above, however, this does not significantly affect the reactivity. The C₇ chains are not strictly linear, with angles at

(48) Balavoine, G.; Collin, J.; Bonnet, J.-J.; Lavigne, G. *J. Organomet. Chem.* **1985**, *280*, 429.

(49) Downard, A. J.; Robinson, B. H.; Simpson, J. *Organomet. Chem.* **1993**, *447*, 281.

(50) Duffy, D. N.; Kassiss, M. M.; Rae, A. D. *Acta Crystallogr., Sect. C* **1991**, *47*, 2054.

(51) Hong, F. E.; Huang, Y.-L.; Cheng, Y.-C.; Chu, K.-M. *Appl. Organomet. Chem.* **2003**, *17*, 458.

(52) Bruce, M. I.; Kramarczuk, K. A.; Perkins, G. J.; Skelton, B. W.; White, A. H.; Zaitseva, N. N. *J. Cluster Sci.* **2004**, *15*, 119.

(53) Bott, S. G.; Yang, K.; Huang, D.-H.; Richmond, M. G. *J. Chem. Crystallogr.* **2004**, *34*, 883.

(54) Blumhofer, R.; Fischer, K.; Vahrenkamp, H. *Chem. Ber.* **1986**, *119*, 194.

(55) Sattelmeyer, K. W.; Stanton, J. F. *J. Am. Chem. Soc.* **2000**, *122*, 8220.

(56) Enkelmann, V. *Chem. Mater.* **1994**, *6*, 1337.

(57) Lu, W.; Xiang, H.-F.; Zhu, N.; Che, C.-M. *Organometallics* **2002**, *21*, 2343.

(58) Bruce, M. I.; Hall, B. C.; Kelly, B. D.; Low, P. J.; Skelton, B. W.; White, A. H. *J. Chem. Soc., Dalton Trans.* **1999**, 3719.

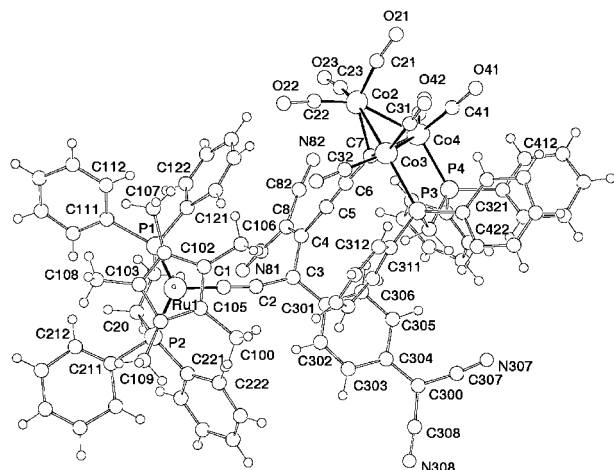


Figure 4. Projection of a molecule of $\{\text{Cp}^*(\text{dppe})\text{Ru}\}\text{C}\equiv\text{CC}(=\text{C}_6\text{H}_4=\text{C}(\text{CN})_2)\text{C}(=\text{C}(\text{CN})_2)\text{C}\equiv\text{CCo}_3(\mu\text{-dppm})(\text{CO})_7$ (**7**) in $7 \cdot 1.25\text{thf}$.

individual carbon atoms ranging between $171.9(7)^\circ$ and $179.0(9)^\circ$ [total bending $\Sigma = 15.6^\circ$ (**1**·thf), 23.8° (**1**·CHCl₃), 27.9° (**2**), 31.3° (**10**), although this is not all in the same sense].

$\{\text{Cp}^*(\text{dppe})\text{Ru}\}\text{C}\equiv\text{CC}[\text{X}=\text{C}(\text{CN})_2]\text{C}(=\text{C}(\text{CN})_2)\text{C}\equiv\text{C}\{\text{Co}_3(\mu\text{-dppm})(\text{CO})_7\}$ ($\text{X} = -\text{6}, \text{C}_6\text{H}_4$ **7**). Projections of these molecules are shown in Figures 4 and 5. It is apparent that the central C(3)–C(4) triple bond in **1** has formally inserted into the C=C double bond of the tcne or tcnq molecule to give tetracyano-diene fragments also attached to the remaining C(1)–C(2) and C(5)–C(6)–C(7) fragments of the C₇ chain. The bridging ligands have the $-\text{C}\equiv\text{C}-\text{C}\{\text{X}=\text{C}(\text{CN})_2\}-\text{C}-$

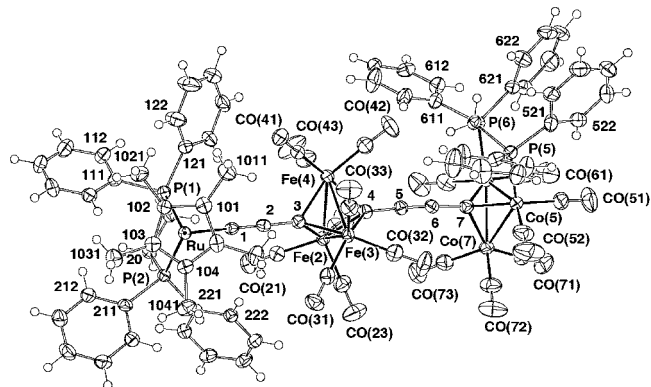


Figure 5. Projection of a molecule of $\{\text{Cp}^*(\text{dppe})\text{Ru}\}\text{C}\equiv\text{CC}[\text{Fe}_3(\text{CO})_9]-\text{CC}\equiv\text{CCo}_3(\mu\text{-dppm})(\text{CO})_7$ (**8**) in $8 \cdot 2\text{C}_6\text{H}_6$.

$\{\text{C}(\text{CN})_2\}-\text{C}\equiv\text{C}-\text{C}\equiv$ formulation ($\text{X} = -\text{6}, \text{C}_6\text{H}_4$ **7**), with two short and three longer C–C separations, the latter consistent with C(sp)–C(sp²) (two) and C(sp²)–C(sp²) single bonds. In **6**, the two dicyanomethylene groups are doubly bonded to C(3) and C(4), while for **7**, C(3) and C(4) are similarly attached to $=\text{C}_6\text{H}_4=\text{C}(\text{CN})_2$ and $=\text{C}(\text{CN})_2$ groups, respectively. Two C≡C triple bonds remain, while C(2)–C(3) and C(4)–C(5) are longer than those in **1** as a result of their being C(sp²)–C(sp) bonds. The C₇ chain is no longer linear, with angles at individual carbon atoms being between $168.1(7)^\circ$ and $177.7(6)^\circ$ for the C(sp) atoms and $116.1(6)^\circ$ and $118.8(6)^\circ$ for C(3, 4), respectively. The dienes adopt the *s-trans* configuration found in the majority of complexes containing this fragment,³¹ as shown by the torsion angles C(30)–C(3)–C(4)–C(40) [$-101.5(8)^\circ$ (**6**), $106(1)^\circ$].

Table 2. Selected Bond Distances and Angles

complex	1 ·2CHCl ₃	1 ·C ₄ H ₈ O	2	6 ·2C ₃ H ₆ O	7 ·1.25thf	8 ·2C ₆ H ₆	8 ·CH ₂ Cl ₂	10 ·0.32C ₆ H ₁₄
Bond Distances (Å)								
Ru–P(1)	2.260(2)	2.263(1)	2.270(2)	2.273(2)	2.306(4)	2.278(1)	2.263(1)	2.285(2)
Ru–P(2)	2.268(2)	2.282(1)	2.263(2)	2.278(2)	2.301(4)	2.296(1)	2.295(1)	2.283(1)
Ru–C(cp)	2.236(8)– 2.274(7)	2.227(4)– 2.277(5)	2.23(1)– 2.272(9)	2.230(6)– 2.292(6)	2.237(14)– 2.326(14)	2.229(5)– 2.272(5)	2.239(4)– 2.266(5)	2.228(5)– 2.268(6)
(av.)	2.259(14)	2.25(3)	2.25(2)	2.26(2)	2.27(3)	2.26(2)	2.25(2)	2.246(15)
Ru–C(1)	1.971(8)	1.971(4)	1.976(7)	1.917(6)	1.88(1)	1.963(4)	1.946(4)	1.960(6)
C(1)–C(2)	1.24(1)	1.241(6)	1.228(8)	1.238(8)	1.23(2)	1.251(6)	1.231(6)	1.239(8)
C(2)–C(3)	1.33(1)	1.348(7)	1.350(8)	1.378(9)	1.42(2)	1.372(6)	1.362(6)	1.362(8)
C(3)–C(4)	1.21(1)	1.232(7)	1.220(7)	1.492(8)	1.51(2)			1.224(8)
C(4)–C(5)	1.36(1)	1.350(7)	1.356(7)	1.403(11)	1.48(2)	1.402(6)	1.370(6)	1.357(8)
C(5)–C(6)	1.22(1)	1.225(7)	1.226(7)	1.200(11)	1.19(2)	1.220(6)	1.218(6)	1.227(8)
C(6)–C(7)	1.40(1)	1.398(7)	1.393(7)	1.387(11)	1.36(2)	1.396(6)	1.370(6)	1.367(8)
C(7)–Co(2)	1.933(7)	1.977(4)	1.950(6)	1.936(6)	1.93(1)	1.944(4)	1.932(4)	1.895(6)
C(7)–Co(3)	1.898(8)	1.903(4)	1.918(5)	1.890(8)	1.93(1)	1.895(5)	1.897(4)	1.912(5)
C(7)–Co(4)	1.902(7)	1.894(5)	1.889(6)	1.904(6)	1.81(1)	1.912(5)	1.905(4)	1.895(5)
Co(2)–Co(3)	2.472(2)	2.4880(8)	2.469(1)	2.472(1)	2.476(2)	2.4968(9)	2.4715(9)	2.381(1)
Co(2)–Co(4)	2.461(2)	2.4740(9)	2.488(1)	2.472(1)	2.465(3)	2.494(1)	2.4927(9)	2.397(1)
Co(3)–Co(4)	2.470(2)	2.4954(9)	2.474(1)	2.463(1)	2.489(3)	2.476(1)	2.4691(9)	2.469(1)
Co(3)–P(3)	2.190(2)	2.208(1)	2.203(2)	2.196(2)	2.241(4)	2.199(2)	2.185(1)	2.214(2)
Co(4)–P(4)	2.188(2)	2.189(1)	2.199(2)	2.188(2)	2.204(4)	2.210(2)	2.206(1)	2.200(2)
Bond Angles (deg)								
P(1)–Ru–P(2)	82.15(8)	82.90(4)	82.11(7)	79.82(6)	85.0(1)	82.53(5)	82.86(4)	83.89(6)
P(1)–Ru–C(1)	89.2(2)	84.6(1)	84.9(2)	85.7(2)	84.0(4)	83.9(2)	82.7(1)	76.8(2)
P(2)–Ru–C(1)	84.7(2)	85.6(1)	92.4(2)	88.6(2)	90.5(1)	90.7(1)	89.9(1)	89.3(2)
Ru–C(1)–C(2)	171.9(7)	176.9(4)	171.6(7)	174.1(6)	176.8(1)	172.4(4)	174.7(4)	172.6(6)
C(1)–C(2)–C(3)	172.1(9)	176.8(5)	173.1(9)	168.1(7)	168.0(1)	179.5(5)	175.8(5)	169.3(8)
C(2)–C(3)–C(4)	179.0(9)	177.8(5)	174.4(9)	116.1(6)	119.1(1)			175.8(9)
C(3)–C(4)–C(5)	178.1(9)	177.6(5)	175.8(8)	118.8(6)	127.0(1)			175.6(6)
C(4)–C(5)–C(6)	178.1(8)	177.6(5)	178.9(8)	176.4(6)	177.6(1)	176.5(6)	175.6(5)	178.2(6)
C(5)–C(6)–C(7)	177.0(8)	177.7(5)	178.3(8)	177.7(6)	172.5(1)	176.4(5)	177.0(5)	177.2(5)
$\Sigma(\text{C}_n)$	23.8	15.6	27.9					31.3
C(6)–C(7)–Co(2)	127.1(5)	121.5(3)	125.2(5)	124.5(5)	125.5(9)	124.8(4)	124.9(3)	128.3(5)
C(6)–C(7)–Co(3)	131.2(6)	134.9(3)	132.8(5)	139.2(5)	124.7(1)	137.4(4)	134.3(3)	132.6(5)
C(6)–C(7)–Co(4)	136.7(6)	137.0(3)	136.7(4)	130.5(4)	140.7(1)	131.5(4)	134.9(3)	136.8(4)

Table 3. Electrochemical Data

compound	#	E ¹	i _c /i _a	E ²	i _c /i _a	E ³	i _c /i _a	ΔE ^{2/3}	E ⁴	i _c /i _a	E ⁵	i _c /i _a
{Ru*}(C≡C) ₃ SiMe ₃		+0.41	0.4									
{Ru*}(C≡C) ₃ {Ru*}		-0.15		+0.33		+1.05		480	+1.33			
{Ru*}(C≡C) ₄ {Ru*}		+0.08		+0.43		+1.07		350	+1.27			
{Ru*}(C≡C) ₂ C{Co ₃ }		-1.33		+0.12		+0.27		150				
{Ru*}(C≡C) ₃ C{Co ₃ }	1	-1.23	1.0	+0.28		+0.39		110	+1.13	0.4		
{Ru*}(C≡C) ₄ C{Co ₃ }		-1.14		+0.42		+0.51		90				
{Ru}(C≡C) ₃ C{Co ₃ }	2	-1.16	0.9	+0.42	0.9	+1.04	0.2					
{Ru'}(C≡C) ₃ C{Co ₃ }		-1.33		+0.22		+0.32		100				
{Ru*}(C≡C) ₃ C{Co ₃ (CO) ₉ }	3	-0.71	0.9	+0.48	0.7	+1.16	irr.					
{Ru*}(C≡C) ₃ C{Co ₃ (dppm)(CO) ₆ (PPh ₃)}	4	-1.26	0.6	+0.17	0.8	+1.06	0.7	890				
{Ru*}(C≡C) ₃ C{Co ₃ Ni}	10	-1.14	1.0	+0.32		+0.48		160	+1.11	0.4		
{Ru*}C≡C(tcne)(C≡C) ₂ C{Co ₃ }	6	-1.10	0.9	-0.78	0.9	+0.78	0.6		+1.16	irr.		
{Ru*}C≡C(tcniq)(C≡C) ₂ C{Co ₃ }	7	-1.38	1.0	-0.66		-0.51			+0.59	irr.	+1.16	irr.
{Ru*}C≡CC{Fe ₃ (CO) ₉ }CC≡CC{Co ₃ }	8	-1.13	1.0	+0.38	0.8	+0.57	0.9	190	+1.37	0.4		
[{Ru*}]=C=CMe(C≡C) ₂ C{Co ₃ }]OTf	5	-0.97	0.9	+0.79	0.3							
{Co ₃ }C(C≡C) ₃ SiMe ₃		-1.33		+0.61								
{Co ₃ }C(C≡C) ₂ C{Co ₃ }		-1.26		-1.11		+0.49		150				
{Co ₃ }C(C≡C) ₄ C{Co ₃ }		-1.03		+0.71								

Addition of tcne or tcniq to the chain occurs at C(3)–C(4), as expected on steric grounds. However, unlike related diyne- and triynyl-ruthenium complexes, no isomeric products formed by addition to either of the other C≡C triple bonds were detected, no doubt as a result of the presence of the bulky Cp* group. This feature contrasts with addition to the C≡C triple bonds that are adjacent to either the Ru center^{30,31} or CO₃ cluster^{23a} that has been observed previously.

{Cp*(dppe)Ru}C≡CC{Fe₃(CO)₉}CC≡CC{Co₃(μ-dppm)(CO)₇} (**8**). XRD structure determinations were carried out on benzene and dichloromethane solvates of **8**. The latter used synchrotron radiation, and values for this determination are cited below (Figure 6). The central C(3)≡C(4) triple bond in **1** has been completely cleaved during the reaction between **1** and Fe₂(CO)₉, which gives **8**. The C≡C triple bonds between C(1)–C(2) and C(5)–C(6) are preserved, but again are somewhat longer than normal C≡C bonds; C(4)–C(5) and C(6)–C(7) correspond to C(sp)–C(sp) single bonds. The C(3)···C(4) separation in **8** is 2.666(6) Å, too long for there to be any residual bonding interaction through the Fe₃ cluster, and the two end groups are sufficiently distant from the central Fe₃ cluster to be unaffected by this part of the molecule, so that the structural parameters are very similar to those of **1**. The trigonal bipyramidal C{Fe₃(CO)₉}C cluster contains an equilateral Fe₃ core [Fe–Fe 2.5189–2.5256(9) Å], with all Fe–C(3,4) bonds being between 1.944 and 2.003(4) Å. Overall, the structure of **8** is similar to those determined earlier for the related complexes {L_mM}C≡CC{Fe₃(CO)₉}C(C≡C)_x{ML_n}, values for similar Fe–C bond lengths being between 1.942(5) and 1.981(8) (ML_n = Fp*, n = 1),³⁸ 1.93(2) and 2.01(3) [ML_n = Ru(dppe)Cp*, x = 1], and 1.96(1) and 2.00(1) Å [ML_n = Ru(dppe)Cp*, x = 2].³⁹

Electrochemistry. The degree of interaction between two redox-active metal end groups through a bridging unit can be probed by electrochemical measurements. Where the end groups are the same or closely related, such as found in the cases of [Cp'(PP)Ru](C≡C)₂[Ru(PP)Cp'] [PP = (PPh₃)(PR₃), R = Me, Ph; dpmm, dppe; Cp' = Cp, Cp*],⁷ electrochemical studies have shown up to four 1-e redox events occur, rather than the intuitively expected two 2-e processes. Computational studies show that the two HOMOs in the neutral complexes undergo stepwise losses of one electron at each stage. Related mononuclear ruthenium complexes may display two 1-e events, as

with Ru(C≡CPh)(dppe)Cp*,⁵⁹ or only one quasi-reversible event, as with Ru{(C≡C)₃SiMe₃}(dppe)Cp*. The cobalt cluster compounds {(OC)_{7-2m}(μ-dppm)_mCo₃}C(C≡C)_xC{Co₃(μ-dppm)_m(CO)_{7-2m}} (m, x = 0, 1) have less pronounced electronic interactions between the capping clusters, each showing two 1-e reduction waves.^{40,41} The compound Co₃{μ₃-C(C≡C)₃SiMe₃}(μ-dppm)(CO)₇ displays one 1-e reduction (–1.33 V) and one 1-e oxidation event (+0.61 V), which is usual for this type of cobalt cluster.⁶⁰

In contrast, when two dissimilar end groups are present, even qualitative analysis of the electronic communication is more complicated than that of the homometallic species. Comparisons of the heterometallic complexes {L_mM}(C≡C)_x{M'L'_n} with the two homometallic series {L_mM}(C≡C)_x{ML_m} and {L'_nM'}(C≡C)_x{M'L'_n} and the monometallic alkynyl derivatives {L_mM}(C≡C)_xR and {L'_nM'}(C≡C)_xR (R = H, Ph, or SiR'₃, for example) may be useful in this regard. Table 3 summarizes the redox potentials that have been determined for the complexes described above, together with other related materials that contain only one of the redox active groups, such as Ru{(C≡C)₃SiMe₃}(dppe)Cp* and Co₃{μ₃-C(C≡C)₃SiMe₃}(μ-dppm)(CO)₇.^{18b}

The cyclic voltammogram (CV) of **1** (Figure 6) displays four redox events, one reduction and three oxidation waves, which might be expected from the presence of two different redox-active metal centers. The reduction E¹ (–1.23 V) was found to be fully reversible, but the two one-electron oxidations E² (+0.28 V) and E³ (+0.39 V) start to merge, making measures of i_A/i_C unreliable. The third oxidation event (E⁴ +1.13 V) is quasi-reversible. Attempts to oxidize **1** to the 1+ and 2+ species chemically were unsuccessful, presumably due to the inherent instability of the system.

The trends observed in the parent homometallic series show that as chain length increases, the electronic interactions between the two Ru termini decrease and their oxidation potentials get higher, while the reduction potential becomes lower in the Co₃ cluster series.^{7b,23a,39} The same changes were also observed with {Cp*(dppe)Ru}{(C≡C)_x-μ₃-C}{Co₃(μ-dppm)(CO)₇} (x = 2, 4).^{18b} Each complex shows four 1-e redox events. In general, as x increases, the difference between the second and third potentials (ΔE^{2/3}) decreases until the two events merge for x =

(59) Cordiner, R. L.; Smith, M. E.; Batsanov, A. S.; Albesa-Jove, A. S.; Hartl, F.; Howard, J. A. K.; Low, P. J. *Inorg. Chim. Acta* **2006**, *359*, 946.

(60) Bruce, M. I.; Cole, M. L.; Gaudio, M.; Skelton, B. W.; White, A. H. J. *Organomet. Chem.* **2006**, *691*, 4601.

Table 4. Crystal Data and Refinement Details

complex	1 • 2CHCl ₃	1 • thf	2	6 • 2Me ₂ CO	7 • 1.25thf	8 • 2C ₆ H ₆	8 • CH ₂ Cl ₂	10 • 0.32C ₆ H ₁₄
formula	C ₇₅ H ₆₁ Co ₃ O ₇ P ₄ Ru • 2CHCl ₃	C ₇₅ H ₆₁ Co ₃ O ₇ P ₄ Ru • C ₄ H ₈ O	C ₇₀ H ₅₁ Co ₃ O ₇ P ₄ Ru	C ₈₁ H ₆₁ Co ₃ N ₄ O ₇ P ₄ Ru • 2C ₃ H ₆ O	C ₈₇ H ₆₅ Co ₃ N ₄ O ₇ P ₄ Ru • 1.25C ₄ H ₈ O	C ₈₄ H ₆₁ Co ₃ Fe ₃ O ₁₆ P ₄ Ru • 2C ₆ H ₆	C ₈₄ H ₆₁ Co ₃ Fe ₃ O ₁₆ P ₄ Ru • CH ₂ Cl ₂	C ₇₇ H ₆₆ Co ₂ NiO ₄ P ₄ Ru • 0.32C ₆ H ₁₄
MW	1714.8	1548.2	1405.9	1720.4	1770.3	2051.9	1980.5	1484.9
cryst syst	monoclinic	orthorhombic	triclinic	monoclinic	monoclinic	triclinic	triclinic	triclinic
space group	<i>P</i> 2 ₁ / <i>c</i>	<i>Ab</i> a2	<i>P</i> 1	<i>P</i> 2 ₁ / <i>c</i>	<i>I</i> 2 ₁ / <i>a</i>	<i>P</i> 1	<i>P</i> 1	<i>P</i> 1
<i>a</i> /Å	21.090(4)	41.252(2)	12.752(2)	22.864(6)	20.468(2)	13.594(1)	11.630(2)	13.406(2)
<i>b</i> /Å	24.169(6)	20.633(2)	14.457(3)	16.392(4)	22.850(3)	15.632(1)	17.055(3)	15.627(2)
<i>c</i> /Å	14.648(6)	16.706(5)	19.409(4)	23.565(6)	35.612(3)	22.940(2)	22.535(4)	18.293(3)
α /deg			111.293(3)			96.484(1)	104.578(5)	84.062(2)
β /deg	96.345(5)		100.089(3)	117.423(4)	102.87(1)	103.045(1)	98.244(5)	75.778(2)
γ /deg			92.221(3)			107.547(1)	105.888(5)	71.231(2)
ρ_s /g cm ⁻³	7421	14219	3262	7839	16237	4441	4051	3516
<i>V</i> /Å ³	1.535	1.446	1.431	1.458	1.448	1.534	1.624	1.402
<i>Z</i>	4	8	2	4	8	2	2	2
$2\theta_{\text{max}}$ /deg	50	62	55	50	50	57	45	52
μ (Mo K α)/mm ⁻¹	1.21	1.04	1.13	0.96	0.90	1.33	0.79	1.08
$T_{\text{min/max}}$	0.86	0.72	0.74	0.82	0.88	0.85	0.76	0.85
cryst dimens/mm ³	0.24 × 0.14 × 0.04	0.47 × 0.38 × 0.12	0.32 × 0.20 × 0.08	0.36 × 0.15 × 0.15	0.16 × 0.04 × 0.04	0.30 × 0.14 × 0.12	0.20 × 0.09 × 0.02	0.55 × 0.21 × 0.13
<i>N</i> _{tot}	61 513	172 680	29 772	46 405	35 342	40 965	79 060	28 392
<i>N</i> (<i>R</i> _{int})	13 207 (0.11)	11 456 (0.047)	15 470 (0.045)	13 691 (0.068)	14 265 (0.24)	21 215 (0.036)	21 134 (0.067)	13 826 (0.036)
<i>N</i> _o	8330	8795	9669	9937	1516	13 634	18 507	13 826
<i>R</i>	0.12	0.045	0.057	0.057	0.090	0.050	0.074	0.047
<i>R</i> _w (<i>n</i> _w)	0.196 (134)	0.076 (34)	0.114 (26)	0.116 (90)	0.16	0.103 (34)	0.061	0.102 (45)
<i>S</i>	1.12	1.34	1.12	1.10	0.98	1.05	1.10	0.90
<i>T</i> /K	150	170	296	150	100	170	110	150

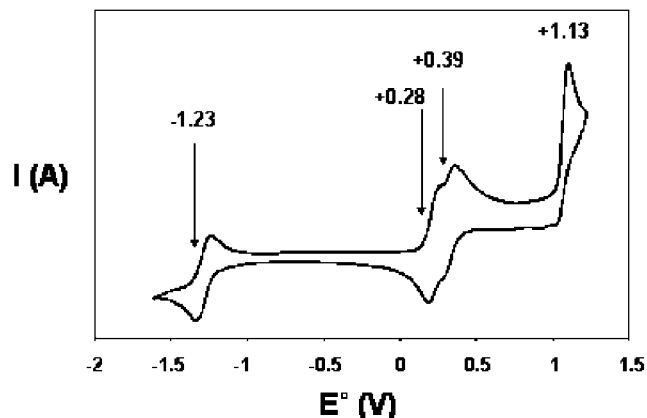


Figure 6. Cyclic voltammogram of $\{Cp^*(dppe)Ru\}[(C\equiv C)_3C]-\{Co_3(\mu-dppm)(CO)_7\}$ (**1**).

4. Each added $C\equiv C$ unit results in an increase in E^1 by ca. 100 mV. The variation in redox potential again suggests that two termini experience a degree of interaction that is attenuated with increasing chain length.

Modification of the metal centers has an obvious effect on the redox potentials of the molecules compared with **1**. Substitution of Cp^* with the less electron donating Cp as in **2** and $\{Cp(PPh_3)_2Ru\}(C\equiv C)_2C\{Co_3(\mu-dppm)(CO)_7\}$ reduces $\Delta E^{2/3}$ to a point where the two 1-e oxidation waves overlap. The electron density in the cobalt cluster can be tuned by substituting electron-withdrawing carbonyl groups by electron-donating phosphine ligands. When one of the carbonyls on the cobalt clusters is replaced by triphenylphosphine, as in **4**, there is no significant effect on the reduction potential ($E^1 -1.26$, cf. -1.23 V for **1**), but the reversibility of the event is reduced. However, the increase in electron density in the molecule results in easier oxidation ($E^2 +0.17$ V), but this event is only quasi-reversible. One further oxidation wave is found at $+1.06$ V. Conversely, removal of all the phosphines in **3** has a more dramatic affect by making the cobalt cluster far easier to reduce at -0.71 V and harder to oxidize, with two events observed at $+0.48$ and $+1.11$ V.

Curiously, substitution of the $Co(CO)_3$ metal fragment in **1** with $NiCp$ in **10** did not change the redox potential noticeably. The second oxidation had a slightly higher potential, marginally increasing $\Delta E^{2/3}$ by 50 mV to 160 mV. Conversely, reduction of **10** is easier than **1** by 90 mV.

Changing the nature of the alkynyl bridging unit also alters the electrochemistry of these molecules. Vinylidene–ruthenium complexes, such as $[Ru(=C=CH_2)(dppe)Cp^*]^+$, have one irreversible process at $+1.68$ V^{7b} and are harder to oxidize because the complex has a positive charge. The methylated compound **5** displays two redox events, an easier 1-e reduction (-0.97 V) and a more difficult oxidation at $+0.79$ V, which has poor reversibility.

The triyne chain is disrupted by formal replacement of one $C\equiv C$ fragment by a tetracyanobutadienediyl group in the *tcn* and *tcnq* adducts **6** and **7**. The cyanocarbon groups are redox active, showing 1-e reductions at -0.78 V (**6**; limited reversibility) and at -0.66 , -0.51 V (**7**; irreversible). The latter result from partial resolution of the effects of the $=C(CN)_2$ and $=C_6H_4=C(CN)_2$ groups. Reversible reduction of the Co_3 cluster occurs at -1.10 V (**6**) and -1.38 V (**7**). Not surprisingly, the electron-withdrawing power of the CN groups is also reflected in the two higher irreversible oxidation events at $+0.78$ and $+1.16$ V (**6**) and $+0.59$ and $+1.16$ V (**7**).

In complex **8** insertion of the $Fe_3(CO)_9$ moiety in the middle of the carbon chain appears to have an electron-withdrawing effect on the molecule as a whole, reduction ($E^1 -1.13$ V) being slightly easier and oxidation ($E^2 +0.38$, $E^3 +0.57$ V) being slightly more difficult when compared to **1**, with $\Delta E^{2/3}$ increasing to 190 mV. In other homometallic $Fe_3(CO)_9$ adducts, for example

$\{Ru(dppe)Cp^*\}C\equiv CC\{Fe_3(CO)_9\}CC\equiv C\{Ru(dppe)Cp^*\}$, the $Fe_3(CO)_9$ core slightly reduces $\Delta E^{1/2}$.³⁹

Although the degree of electronic communication between the two metal termini in **1** cannot be quantified, the above results show that changes in electron density in each of the end groups and in the C_7 chain are reflected in the CVs of the various derivatives. In turn, this suggests that a variable degree of electronic interaction occurs along the C_7 chain. Further quantification of these effects must await more detailed spectro-electrochemical and computational studies.

Conclusions

A variety of synthetic approaches is now available to construct complexes in which carbon chains of various lengths are end-capped by various metal–ligand moieties. We have applied these methodologies to the syntheses of **1**, **2**, and **3**, which contain $Ru(dppe)Cp'$ ($Cp' = Cp^*, Cp$) and $Co_3(\mu-dppm)_n(CO)_{9-2n}$ ($n = 1, 0$) end groups linked by C_7 chains. The reactions of **1** with several reagents give products that are in accord with the normal reactivity of the components of this complex, such as the formation of a substituted vinylidene attached to the ruthenium center, addition of *tcn*, *tcnq*, or $Fe_3(CO)_9$ groups to the central $C\equiv C$ triple bond, or Co replacement by Ni in the Co_3 cluster. This pattern of reactivity found for **1** suggests that in this complex the C_7 chain is long enough to prevent any significant modification of the characteristic reactions of one end group by the other. However, direction of reactions to the central $C\equiv C$ triple bond of the C_7 chain results from steric effects of the diphosphine ligand, specifically the phenyl groups thereof, attached to the metal centers at each end of the carbon chain.

Experimental Section

General Comments. All reactions were carried out under dry high-purity nitrogen using standard Schlenk techniques unless otherwise stated, although normally no special precautions to exclude air were taken during the subsequent workup. Common solvents were dried, distilled under nitrogen, and degassed before use. Separations were carried out by preparative thin-layer chromatography (TLC) on glass plates (20×20 cm) coated with silica (Merck 60 GF254, 0.5 mm thick). Flash column chromatography was performed using silica (Scharlau 60, 0.04–0.06 mm, 230–400 mesh) or basic alumina (Fluka, Brockmann activity II, basic, pH 10 ± 0.5).

Instruments. IR spectra were obtained on a Perkin-Elmer Spectrum BX FT-IR infrared spectrometer. Spectra in CH_2Cl_2 were obtained using a 0.5 mm path length solution cell with NaCl windows. Nujol mull spectra were obtained from samples mounted between NaCl disks. NMR spectra were recorded on a Varian Gemini 2000 (1H at 199.98 MHz, ^{13}C at 50.29 MHz), Varian Gemini 3000 (1H at 300.15 MHz, ^{13}C at 75.47 MHz, ^{31}P at 121.105 MHz), or Varian Inova 600 spectrometer (^{13}C at 150.87 MHz). Unless otherwise stated, samples were dissolved in $CDCl_3$ or C_6D_6 (Sigma-Aldrich), contained in 5 mm sample tubes. Chemical shifts are given in ppm relative to internal tetramethylsilane for 1H and ^{13}C NMR spectra and external H_3PO_4 for ^{31}P NMR spectra. Electrospray mass spectra (ES-MS) were obtained from samples

dissolved in MeOH unless otherwise indicated. Solutions were injected into a Varian Platform II spectrometer via a 10 mL injection loop. Ions listed are the most intense peaks in the isotopic envelope. Nitrogen was used as the drying and nebulizing gas. Added NaOMe was used as an aid to ionization.⁶¹

Electrochemical samples (1 mM) were dissolved in CH₂Cl₂ containing 0.1 M [NBu₄]PF₆ as the supporting electrolyte. Cyclic voltammograms were recorded using a PAR model 263A potentiostat, with a saturated calomel electrode. The cell contained a Pt-mesh working electrode and Pt wire counter and pseudoreference electrodes. Potentials are given in V vs SCE, with ferrocene as internal calibrant (FeCp₂/[FeCp₂]⁺ = +0.46 V). Microanalyses were by CMAS, Belmont, Vic., Australia.

Reagents. The compounds Co₃(μ₃-CBr)(μ-dppm)(CO)₇,⁵² Co₃(μ₃-CBr)(CO)₉,⁶² Co₃{μ₃-C(C≡C)_xAu(PPh₃)₃}(μ-dppm)(CO)₇ (x = 1, 2),¹⁸ Ru{(C≡C)₂R}(dppe)Cp* [R = H, Au(PPh₃)],⁶³ [Ru(=C=CH₂)(dppe)Cp']PF₆ (Cp' = Cp, Cp*),⁶⁴ AuCl(PPh₃),⁶⁵ [(py)₂]BF₄,⁶⁶ and Pd(PPh₃)₄⁶⁷ were prepared by standard literature procedures. All other reagents were obtained as described below, or from Sigma-Aldrich or Fluka and used without further purification.

Me₃SiC≡CI. LiBu (1.6 M solution in hexane, 9.4 mL, 15 mmol) was added to HC≡CSiMe₃ (2 mL, 15 mmol) in Et₂O (40 mL) at -40 °C, and the mixture was stirred for 5 min. A solution of I₂ (ca. 2 g) in Et₂O was added slowly until the brown color persisted, and the mixture was stirred for a further 10 min before being washed with aqueous Na₂S₂O₃ (4 × 50 mL) and saturated aqueous NaCl (2 × 50 mL). The organic layer was separated, dried (MgSO₄), and evaporated (0 °C) in a Al-foil-covered flask to give Me₃SiC≡CI (1.54 g, 46%), identified by ¹H NMR (CDCl₃) [δ 0.18 (s, 9H, SiMe₃)] and ¹³C NMR [δ 0.10 (s, SiMe₃), 0.22 (s, C≡CI), 104.41 (s, C≡CSiMe₃)].

Ru{(C≡C)₃SiMe₃}(dppe)Cp*. A solution of Me₃SiC≡CI (268 mg, 1.20 mmol) in degassed thf (25 mL) was added to a Schlenk flask containing Ru{(C≡C)₂Au(PPh₃)}(dppe)Cp* (660 mg, 0.577 mmol), Pd(PPh₃)₄ (20 mg, 0.017 mmol), and CuI (6.4 mg, 0.034 mmol), and the solution was stirred for 16 h at rt. The solvent was removed under reduced pressure, and the resulting residue was taken up in the minimum amount of triethylamine and purified by chromatography (basic alumina, hexane-triethylamine, 4:1). Solvent was removed from the first yellow fraction product to afford Ru{(C≡C)₃SiMe₃}(dppe)Cp* as a yellow solid (376 mg, 83%). Anal. Calcd (C₄₅H₄₈P₂RuSi): C, 69.21; H, 6.20; M, 781. Found: C, 69.28; H, 6.31. IR (Nujol, cm⁻¹): ν(C≡C) 2110s, 1971s. ¹H NMR (C₆D₆): δ 0.11 (s, 9H, SiMe₃), 1.50 (s, 15H, Cp*), 1.63–1.85, 2.30–2.51 (2 × m, 2 × CH₂), 7.00–7.24, 7.70–7.76 (2 × m, 20H, Ph). ¹³C NMR (C₆D₆): δ 0.21 (s, SiMe₃), 10.05 (s, C₅Me₅), 28.78–29.94 (m, CH₂), 49.43, 69.79, 77.93, 92.19, 94.09 (5 × s, C), 93.90 [t, ²J(CP) 2.0 Hz, C₅Me₅], 137.58 [t, J(CP) = 23 Hz, C(1)], 128.29–138.38 (m, Ph). ³¹P NMR (C₆D₆): δ 80.4 (s, Ru-dppe). ES-MS (positive ion mode, MeOH, m/z): 781, M⁺; 635, [Ru(dppe)Cp*]⁺.

Ru{(C≡C)₃Au(PPh₃)}(dppe)Cp*. A methanolic solution of NaOMe was prepared by the addition of Na (20 mg, 0.87 mmol) to degassed MeOH (10 mL). Once the effervescence had ceased,

Ru{(C≡C)₃SiMe₃}(dppe)Cp* (338 mg, 0.433 mmol) was added to the solution and allowed to stir for 15 min. AuCl(PPh₃) (214 mg, 0.433 mmol) was added, and stirring was continued for a further 3 h. The yellow precipitate was collected on a sintered filter and washed with MeOH (2 × 5 mL) and hexane (5 mL) to afford Ru{(C≡C)₃Au(PPh₃)}(dppe)Cp* as a yellow solid (475 mg, 94%). Anal. Calcd (C₆₀H₅₄AuP₃Ru): C, 61.80; H, 4.67; M, 1166. Found: C, 61.90; H, 4.59. IR (Nujol, cm⁻¹): ν(C≡C) 2121m, 2088w, 1965m. ¹H NMR (C₆D₆): δ 1.54 (s, 15H, Cp*), 2.01–2.25, 2.56–2.79 (2 × m, 2 × CH₂), 7.17–7.70 (m, 35H, Ph). ¹³C NMR (CDCl₃): δ 10.19 (s, C₅Me₅), 28.98–30.05 (m, CH₂), 48.99, 51.19, 64.41, 92.01, 94.15, 154.43 (6 × s, C), 93.79 (s, C₅Me₅), 127.62–138.38 (m, Ph). ³¹P NMR (C₆D₆): δ 80.9 (s, 2P, Ru-dppe), 42.4 (s, 1P, Au-PPh₃). ES-MS (positive ion mode, MeOH–NaOMe, m/z): 1189, [M + Na]⁺; 721, [Au(PPh₃)₂]⁺; 635, [Ru(dppe)Cp*]⁺.

{Cp*(dppe)Ru}{(C≡C)₃-μ₃-C}{Co₃(μ-dppm)(CO)₇} (**1**). **Method a.** A solution of Ru{(C≡C)₃Au(PPh₃)}(dppe)Cp* (461 mg, 0.395 mmol), Co₃(μ₃-CBr)(μ-dppm)(CO)₇ (335 mg, 0.395 mmol), Pd(PPh₃)₄ (40 mg, 0.032 mmol), and CuI (9 mg, 0.051 mmol) in degassed thf (50 mL) was stirred for 16 h. The solvent was removed under reduced pressure and purified by preparative TLC (acetone–hexane, 3:7) to give a brown band (R_f = 0.55), which was further separated by preparative TLC (CH₂Cl₂–hexane, 1:1) into three bands. The fastest moving brown band (R_f = 0.60) contained {(CO)₇(μ-dppm)Co₃}{μ₃-μ₃-C(C≡C)₂C} (12 mg, 4%), identified spectroscopically and by XRD (crystals from CH₂Cl₂–hexane). The middle brown band (R_f = 0.50) afforded {Cp*(dppe)Ru}{(C≡C)₃-μ₃-C}{Co₃(μ-dppm)(CO)₇} (**1**) as a brown solid (196 mg, 34%). The lower brown band (R_f = 0.40) contained **1** together with AuBr(PPh₃) [³¹P NMR: δ 35.7 (C₆D₆), 36.4 (CDCl₃)], which was removed by column chromatography (silica gel, toluene). The first fraction contained **1** (107 mg, 18%; total yield 303 mg, 52%). X-ray quality crystals were grown from thf–MeOH or CHCl₃–MeOH. Anal. Calcd (C₇₅H₆₁Co₃O₇P₄Ru): C, 61.03; H, 4.17; M, 1476. Found: C, 61.02; H, 3.98. IR (CH₂Cl₂, cm⁻¹): ν(CO) 2079w, 2053m, 2008m, 1941m. ¹H NMR (C₆D₆): δ 1.56 (s, 15H, Cp*), 1.75–1.98, 2.69–2.95 (2 × m, 2 × CH₂, dppe), 2.96–3.14, 4.40–4.63 (2 × m, CH₂, dppm), 6.70–7.82 (m, 40H, Ph). ¹³C NMR (CDCl₃): δ 9.68 (s, C₅Me₅), 28.88–29.80 (m, CH₂, dppe), 40.32–41.46 (m, CH₂, dppm), 48.79, 90.70, 91.49, 94.85, 104.01, 151.88 (6 × s, C), 93.83 (s, C₅Me₅), 127.26–137.60 (m, Ph), 201.96 (m, CO). ³¹P NMR (C₆D₆): δ 33.9 (s, 2P, Co₃-dppm), 80.2 (s, 2P, Ru-dppe). ES-MS (positive ion mode, MeOH–NaOMe, m/z): 1499, [M + Na]⁺; 1476, M⁺; 1448, [M – CO]⁺.

Method b. To a solution of [Ru(=C=CH₂)(dppe)Cp']PF₆ (80 mg, 0.10 mmol) in thf (30 mL) at -78 °C was added BuLi (0.08 mL, 2.5 M in hexane, 0.20 mmol), and the mixture was stirred for 30 min. The flask was protected from light with aluminum foil, solid [(py)₂]BF₄ (38 mg, 0.10 mmol) was then added, and stirring was continued for a further 1 h. The solution was transferred by cannula to a foil-wrapped Schlenk flask containing Co₃(μ₃-C(C≡C)₂Au(PPh₃))(μ-dppm)(CO)₇ (85 mg, 0.066 mmol), Pd(PPh₃)₄ (10 mg, 0.008 mmol), and CuI (2 mg, 0.01 mmol). The solution was left to stir at rt for 24 h, and the purification protocol for (a) above was employed to give **1** as a brown solid (25 mg, 26%).

Method c (i). To a solution of Ru{(C≡C)₂H}(dppe)Cp* (231 mg, 0.305 mmol) in thf (25 mL) at -78 °C was added BuLi (0.12 mL, 2.5 M in hexane, 0.305 mmol), and the mixture was stirred for 30 min. The flask was protected from light with aluminum foil, solid [(py)₂]BF₄ (113 mg, 0.305 mmol) was added, and stirring was continued for a further 1 h. The solution was transferred by cannula to a foil-wrapped Schlenk flask containing Co₃(μ₃-CC≡CAu(PPh₃))(μ-dppm)(CO)₇ (301 mg, 0.240 mmol), Pd(PPh₃)₄ (30 mg, 0.024 mmol), and CuI (4 mg, 0.022 mmol). The solution was left to stir at rt for 24 h, and the purification protocol for (a) above was employed to afford **1** as a brown solid (202 mg, 57%).

(61) Henderson, W.; McIndoe, J. S.; Nicholson, B. K.; Dyson, P. J. *J. Chem. Soc., Dalton Trans.* **1998**, 519.

(62) Ercoli, R.; Santambrogio, E.; Casagrande, G. *Chim. Ind. (Milan)* **1962**, *44*, 1344.

(63) Bruce, M. I.; Ellis, B. G.; Gaudio, M.; Lapinte, C.; Melino, G.; Paul, F.; Skelton, B. W.; Smith, M. E.; Toupet, L.; White, A. H. *Dalton Trans.* **2004**, 1601.

(64) Bruce, M. I.; Costuas, K.; Ellis, B. G.; Halet, J.-F.; Low, P. J.; Moubarak, B.; Murray, K. S.; Ouddaï, N.; Perkins, G. J.; Skelton, B. W.; White, A. H. *Organometallics* **2007**, *26*, 3735.

(65) Bruce, M. I.; Nicholson, B. K.; bin Shawkataly, O. *Inorg. Synth.* **1989**, *26*, 324.

(66) Barluenga, J.; Rodriguez, M. A.; Campos, P. J. *J. Org. Chem.* **1990**, *55*, 3104.

(67) Coulson, D. R. *Inorg. Synth.* **1990**, *28*, 107.

Method c (ii). To a solution of Ru{(C≡C)₂SiMe₃}(dppe)Cp* (90 mg, 0.120 mmol) in thf (25 mL) at -78 °C was added LiMe (0.08 mL, 1.5 M in diethyl ether, 0.120 mmol), and the mixture was stirred for 1 h. The flask was protected from light with aluminum foil, and solid [(py)₂]BF₄ (44 mg, 0.120 mmol) was added. Stirring was continued for a further 1 h, and the solution was transferred by cannula to a light-protected Schlenk flask containing Co₃{μ₃-CC≡CAu(PPh₃)}(μ-dppm)(CO)₇ (100 mg, 0.080 mmol), Pd(PPh₃)₄ (20 mg, 0.016 mmol), and CuI (4 mg, 0.022 mmol). The solution was left to stir at rt for 24 h, and the purification protocol for (a) above was employed to afford **1** as a brown solid (12 mg, 10%).

Extra care to exclude air, moisture, and light from reaction mixtures involving Ru{(C≡C)_nI}(dppe)Cp' (where *n* = 1 or 2 and Cp' = Cp* or Cp) was necessary, due to the sensitivity of these compounds.

{Cp(dppe)Ru}{(C≡C)₃-μ₃-C}{Co₃(μ-dppm)(CO)₇} (2). As in (b) above, the reaction between [Ru(=C=CH₂)(dppe)Cp]PF₆ (81 mg, 0.11 mmol), BuLi (0.09 mL, 2.5 M in hexane, 0.22 mmol), [(py)₂]BF₄ (41 mg, 0.11 mmol), Co₃{μ₃-C(C≡C)₂Au(PPh₃)}(μ-dppm)(CO)₇ (93 mg, 0.07 mmol), Pd(PPh₃)₄ (10 mg, 0.008 mmol), and CuI (2 mg, 0.01 mmol) gave a brown residue, which was purified by preparative TLC (acetone-hexane, 3:7, *R_f* = 0.5 and CH₂Cl₂-hexane, 1:1, *R_f* = 0.4) to give {Cp(dppe)Ru}{(C≡C)₃-μ₃-C}{Co₃(μ-dppm)(CO)₇} (**2**) as a dark brown solid (27 mg, 26%). X-ray quality crystals were obtained from CH₂Cl₂-hexane. Anal. Calcd (C₇₀H₅₁Co₃O₇P₄Ru): C, 59.80; H, 3.66; *M*, 1406. Found: C, 59.75; H, 3.65. IR (CH₂Cl₂): ν(CO) 2084w, 2054s, 2007s, 1950m cm⁻¹. ¹H NMR (C₆D₆): δ 1.98–2.26, 2.50–2.74 (2 × m, 2 × CH₂, dppe), 3.17, 4.51 (2 × m, CH₂, dppm), 4.18 (s, 5H, Cp), 6.86–8.04 (m, 40H, Ph). ¹³C NMR (C₆D₆): δ 27.47–31.34 (m, dppe), 40.13–40.77 (m, dppm), 83.40 (s, Cp), 126.98–137.84 (m, Ph). ³¹P NMR (C₆D₆): δ 34.0 (s, 2P, Co₃-dppm), 85.1 (s, 2P, Ru-dppe). ES-MS (positive ion mode, MeOH-NaOMe, *m/z*): 1429, [M + Na]⁺; 1406, M⁺.

{Cp*(dppe)Ru}{(C≡C)₃-μ₃-C}{Co₃(CO)₉} (3). Tetrahydrofuran (20 mL) was added to a Schlenk flask containing Ru{(C≡C)₃Au(PPh₃)}(dppe)Cp* (21 mg, 0.018 mmol), Co₃(μ₃-CBr)(CO)₉ (10 mg, 0.018 mmol), Pd(PPh₃)₄ (5 mg, 0.004 mmol), and CuI (2 mg, 0.01 mmol). After 40 min the solvent was removed under reduced pressure and the residue purified by preparative TLC (acetone-hexane, 3:7, *R_f* = 0.75), which gave {Cp*(dppe)Ru}{(C≡C)₃-μ₃-C}{Co₃(CO)₉} (**3**) as a dark maroon solid (15 mg, 48%). IR (CH₂Cl₂, cm⁻¹): ν(CO) 2075w, 2052s, 1967w, 1922m. ¹H NMR (CDCl₃): δ 1.56 (s, 15H, Cp*), 1.76, 2.40 (2 × m, 2 × CH₂, dppe), 7.02–7.74 (m, 20H, Ph). ¹³C NMR (C₆D₆): δ 10.51 (C₅Me₅), 29.66–30.60 (m, dppe), 94.82 (s, C₅Me₅), 127.06–134.02 (m, Ph), 200.58 (m, CO). ³¹P NMR (CDCl₃): δ 79.7 [s, 2P, Ru(dppe)]. ES-MS (negative ion mode, MeOH-NaOMe, *m/z*): 1179, [M + OMe]⁻ (calcd *M*, 1148). Consistent microanalytical data could not be obtained for **3**.

Reactions of {Cp*(dppe)Ru}{(C≡C)₃-μ₃-C}{Co₃(μ-dppm)(CO)₇} (1).

(a) With triphenylphosphine and TMNO. To a stirred solution of **1** (50 mg, 0.034 mmol) and PPh₃ (9 mg, 0.034 mmol) in thf (20 mL) was added TMNO (3 mg, 0.034 mmol). After stirring for 1 h at rt, the reaction mixture was heated at reflux for 16 h. Solvent was removed under reduced pressure, and the crude material was purified by preparative TLC (acetone-hexane, 3:7; *R_f* = 0.45) to give {Cp*(dppe)Ru}{(C≡C)₃-μ₃-C}{Co₃(μ-dppm)(PPh₃)(CO)₆} (**4**) as a brown-black solid (24 mg, 41%). Anal. Calcd (C₉₂H₇₆Co₃O₆P₅Ru): C, 64.61; H, 4.48; *M*, 1710. Found: C, 64.73; H, 4.54. IR (CH₂Cl₂, cm⁻¹): +ν(CO) 2078w, 2020m, 1988m, 1968w, 1945m. ¹H NMR (CDCl₃): δ 1.64 (s, 15H, Cp*), 2.12–2.38, 2.69–2.95 (2 × m, 2 × CH₂, dppe), 3.21–3.42, 4.40–4.63 (2 × m, CH₂, dppm), 7.11–7.82 (m, 55H, Ph). ¹³C NMR (CDCl₃): δ 10.34 (C₅Me₅), 29.54 (br, dppe), 94.27 (s, C₅Me₅), 127.94–137.58 (m, Ph), 202.23 (m, CO). ³¹P NMR (CDCl₃): δ 33.6 [br d, *J*(PP)

= 39 Hz, 2P, Co₃-dppm], 48.4 (br, 1P, Co₃-PPh₃), 80.5 (s, 2P, Ru-dppe). ES-MS (positive ion mode, MeOH-NaOMe, *m/z*): 1733, [M + Na]⁺.

Alternatively, a stirred solution of **1** (32 mg, 0.022 mmol) and PPh₃ (11 mg, 0.041 mmol) in thf (15 mL) was heated at reflux for 3 h. Solvent was removed under reduced pressure and the crude material purified by preparative TLC (acetone-hexane, 3:7, *R_f* = 0.45). The reaction gave {Cp*(dppe)Ru}{(C≡C)₃-μ₃-C}{Co₃(μ-dppm)(PPh₃)(CO)₆} as a brown-black solid (31 mg, 84%).

(b) With methyl triflate. A stirred solution of **1** (100 mg, 0.0678 mmol) in CH₂Cl₂ (10 mL) was cooled to -78 °C and treated with MeOTf (11.1 mg, 0.068 mmol). After 90 min, the solution was allowed to warm to rt. After 5 days, the reaction mixture was run through a squat silica column, first eluting with acetone-hexane (1:4) to recover **1** (47 mg) and then with acetone-hexane (4:1) to give [{Cp*(dppe)Ru}C≡CMe(C≡C)₂C-Co₃(μ-dppm)(CO)₇]OTf (**5**) as a brown solid (37 mg, 63% conversion). Anal. Calcd (C₇₇H₆₄Co₃O₁₀F₄RuF₃S): C, 56.39; H, 3.93; *M* (cation), 1491. Found: C, 56.22; H, 4.03. IR (CH₂Cl₂, cm⁻¹): +ν(CO) 2060m, 2010s, ν(C=C) 1603w, 1435w. ¹H NMR (*d*₆-acetone): δ 1.28 (s, 3H, Me), 1.83 (s, 15H, Cp*), 2.53, 3.10 (2 × m, 2 × CH₂, dppe), 4.17, 4.63 (2 × m, CH₂, dppm), 7.21–7.74 (m, 40H, Ph). ¹³C NMR (*d*₆-acetone): δ 10.15 (s, Me) 10.52 (s, C₅Me₅), 44.96 (m, dppm), 81.51, 91.04, 97.32, 107.56, 109.04 (5 × s, C), 105.24 (s, C₅Me₅), 128.70–135.85 (m, Ph), 203.16 (br, CO), 215.09 (br, CCo₃), 357.39 [t, ²*J*(CP) = 16 Hz, Ru=C]. ³¹P NMR (*d*₆-acetone): δ 34.9 (s, 2P, Co₃-dppm), 74.0 (s, 2P, Ru-dppe). ES-MS (positive ion mode, MeOH, *m/z*): 1491, M⁺; 663, [Ru(CO)(dppe)Cp*]⁺.

(c) With tcne. C₂(CN)₄ (5 mg, 0.034 mmol) was added to a stirred solution of **1** (50 mg, 0.034 mmol) in CH₂Cl₂ (15 mL). After 30 s the solution turned from dark brown to purple, and after 5 min the solution was black. After 30 min solvent was removed under reduced pressure and the black residue was purified by preparative TLC (CH₂Cl₂, *R_f* = 0.6), to give {Cp*(dppe)Ru}C≡CC[=C(CN)₂]C[=C(CN)₂]C≡C-μ₃-C{Co₃(μ-dppm)(CO)₇} (**6**) as a black solid (42 mg, 77%). X-ray quality crystals were obtained from acetone-hexane. Anal. Calcd (C₈₁H₆₁Co₃N₄O₇P₄Ru): C, 60.65; H, 3.83; N, 3.49; *M*, 1604. Found: C, 60.61; H, 3.89; N, 3.48. IR (CH₂Cl₂, cm⁻¹): ν(CN) 2210w, +ν(CO) 2077m, 2043s, 2025s, 1962s, ν(C=C) 1507w, 1464w, 1436w. ¹H NMR (C₆D₆): δ 1.56 (s, 15H, Cp*), 1.97–2.21, 2.53–2.78 (2 × m, 2 × CH₂, dppe), 4.25–4.39, 4.40–4.62 (2 × m, CH₂, dppm), 6.66–7.88 (m, 40H, Ph). ¹³C NMR (C₆D₆): δ 9.91 (C₅Me₅), 29.31–30.12 (m, dppe), 40.13–40.77 (m, dppm), 75.43, 83.65, 105.56, 139.21, 142.90, 151.03 (6 × s, C), 96.87 (s, C₅Me₅), 113.63, 113.90, 116.64, 116.83 (4 × s, CN) 127.63–134.25 (m, Ph), 201.82 (m, CO), 216.58 (m, CCo₃). ³¹P NMR (C₆D₆): δ 34.5, 35.3 [AB q, *J*(PP) = 47 Hz, 2P, Co₃-dppm], 80.0, 80.3 [AB q, *J*(PP) = 10 Hz, 2P, Ru-dppe]. ES-MS (positive ion mode, MeOH-NaOMe, *m/z*): 1627, [M + Na]⁺; 1604, M⁺.

(d) With tcnq. To a stirred solution of **1** (40 mg, 0.027 mmol) in CH₂Cl₂ (15 mL) was added tcnq (6 mg, 0.030 mmol). After 5 min the solution turned from dark brown to dark green and after 15 min was dark blue. After 75 min the solvent was removed under reduced pressure and the blue residue was taken up in CH₂Cl₂ and loaded onto a silica column (10 cm). It was first eluted with CH₂Cl₂ to remove a yellow impurity and then with acetone-hexane (3:7) to give a blue fraction containing {Cp*(dppe)Ru}C≡CC[=C₆H₄=C(CN)₂]C[=C(CN)₂]C≡CC-μ₃{Co₃(μ-dppm)(CO)₇} (**7**), obtained as a dark blue solid (39 mg, 86%). X-ray quality crystals were obtained from thf-MeOH. Anal. Calcd (C₈₇H₆₅Co₃N₄O₇P₄Ru.1.5CH₂Cl₂): C, 59.08; H, 3.66; N, 2.81; *M*, 1680. Found: C, 58.80; H, 3.79; N, 2.81. IR (cm⁻¹, CH₂Cl₂): ν(CN) 2193w, ν(CO) 2076w, 2044s, 2018vs, 1949br m, ν(C=C) 1585br m, 1369br m cm⁻¹. ¹H NMR (C₆D₆): δ 1.43 (s, 15H, Cp*), 1.95–2.19, 2.59–2.81 (2 × m, 2 ×

CH₂, dppe), 3.23–3.37, 4.11–4.26 (2 × m, CH₂, dppm), 4.28 (s, 3H, CH₂Cl₂), 6.18, 6.21 (2 × s, =CH), 6.63–7.61 (m, 44H, Ph). ¹³C NMR (C₆D₆): δ 10.01 (C₅Me₅), 28.95–30.09 (m, PCH₂CH₂P), 39.88–40.50 (m, PCH₂P), 53.33 (s, CH₂Cl₂), 63.24, 82.70, 108.56, 154.39, 155.33 (5 × s, C), 96.62 (s, C₅Me₅), 114.24, 115.44, 117.92, 118.12 (4 × s, CN) 122.33–141.10 (m, Ph), 201.62 (2 × m, CO). ³¹P NMR (C₆D₆): δ 33.3 [br s, 2P, dppm], 79.6 [br d, J(PP) = 369 Hz, 2P, dppe]. ES-MS (positive ion mode, MeOH–NaOMe, *m/z*): 1703, [M + Na]⁺; 1680, M⁺.

(e) **With Fe₂(CO)₉**. Solvent (thf or benzene) was added to a flask containing Fe₂(CO)₉ (about 10 equiv) and {Cp*(dppe)Ru}-(C≡C)₃C{Co₃(μ-dppm)(CO)₇}, and the mixture was stirred for the appropriate period. The solution was then filtered through a short column of flash silica, and the crude mixture was purified by preparative TLC (acetone–hexane, 3:7).

The mixture in thf was heated to reflux for 80 min, the solution turning from brown to dark green-brown. At this point, spot TLC revealed that the starting material had been consumed. Purification by preparative TLC gave purple {Cp*(dppe)Ru}C≡CC{Fe₃(CO)₉}-CC≡CC{Co₃(μ-dppm)(CO)₇} (**8**) (12 mg, 9%) and green-brown {Cp*(dppe)Ru}-(C≡C)₃C{Co₃(μ-dppm)(CO)₇}{Fe₂(CO)₆} (**9**) (25 mg, 21%). Similar reactions carried out (a) at rt in thf for 5 h afforded **8** (24%) and **9** (13%); (b) at rt in benzene for 3 h gave **8** (28 mg, 29%) and an unidentified ochre compound (8 mg).

{Cp*(dppe)Ru}C≡CC{Fe₃(CO)₉}CC≡CC{Co₃(μ-dppm)(CO)₇} (**8**). X-ray quality crystals were obtained from C₆D₆–MeOH. Anal. Calcd (C₈₄H₆₁Co₃Fe₃O₁₆P₄Ru): C, 53.22; H, 3.24; *M*, 1896. Found: C, 53.30; H, 3.19. IR (CH₂Cl₂, cm⁻¹): ν(CO) 2069w, 2052m, 2031s, 1999m, 1913m. ¹H NMR (C₆D₆): δ 1.63 (s, 15H, Cp*), 1.84–2.02, 2.59–2.77 (2 × m, 2 × CH₂, dppe), 3.15–3.22, 4.60–4.66 (2 × m, CH₂, dppm), 7.08–7.76 (m, 40H, Ph). ¹³C NMR (C₆D₆): δ 11.05 (s, C₅Me₅), 29.91–30.96 (m, dppe), 38.70–39.96 (m, dppm) 80.50, 92.90, 114.09, 154.78 (4 × s, C), 96.36 (s, C₅Me₅), 126.78–142.02 (m, Ph), 203.18 (br, Co–CO), 211.95 (s, Fe–CO), 252.61, 273.10 (2 × s, CFe₃). ³¹P NMR (C₆D₆): δ 35.2 (s, 2P, Co₃-dppm), 78.5 (s, 2P, Ru-dppe). ES-MS (positive ion mode, MeOH–NaOMe, *m/z*): 1918, [M + Na]⁺; 1896, M⁺.

{Cp*(dppe)Ru}-(C≡C)₃C{Co₃(μ-dppm)(CO)₇}{Fe₂(CO)₆} (**9**). Anal. Calcd (C₈₁H₆₁Co₃Fe₂O₁₃P₄Ru·CH₂Cl₂): C, 53.50; H, 3.45; *M*, 1756. Found: C, 53.27; H, 4.05. IR (CH₂Cl₂, cm⁻¹): ν(CO) 2070w, 2042s, 2029m, 2011m, 1995s. ¹H NMR (C₆D₆): δ 1.64 (s, 15H, Cp*), 1.96–2.07, 2.68–2.85 (2 × m, 2 × CH₂, dppe), 3.08–3.15, 3.40–4.46 (2 × m, CH₂, dppm), 4.28 (s, 2H, CH₂Cl₂), 6.92–7.84 (m, 40H, Ph). ³¹P NMR (C₆D₆): major isomer (65%) δ 48.2 [br d, J(PP) = 121 Hz, Co₃-dppm], 81.0, 81.2 [AB quartet, J(PP) = 23 Hz, Ru-dppe]; minor isomer (35%) 54.0 [br d, J(PP) = 145 Hz, Co₃-dppm], 80.2, 82.5 [AB quartet, J(PP) = 283 Hz, Ru-dppe]. ES-MS (positive ion mode, MeOH–NaOMe, *m/z*): 1779, [M + Na]⁺; 1756, M⁺.

(f) **With NiCp₂**. A mixture of **1** (50 mg, 0.034 mmol) and NiCp₂ (14 mg, 0.075 mmol) was stirred in thf (20 mL) at rt for 1 h and at reflux for 16 h. Solvent was removed under reduced pressure and the residue was purified by preparative TLC (acetone–hexane, 3:7) to give {Cp*(dppe)Ru}C≡CC≡CC≡CC{Co₂Ni(μ-dppm)(CO)₄Cp} (**10**) (24 mg, 41%) as a brown solid. Crystals suitable for X-ray diffraction were grown from acetone–hexane. Anal. Calcd (C₇₇H₆₆Co₂NiO₄P₄Ru): C, 63.48; H, 4.57; *M*, 1456. Found: C, 63.10; H, 4.37. IR (CH₂Cl₂, cm⁻¹): ν(CO) 2076w, 2005w, 1983m, 1960 (sh), 1939m. ¹H NMR (C₆D₆): δ 1.57 (s, 15H, Cp*), 2.03, 2.74 (2 × m, 2 × CH₂, dppe), 3.09, 4.25 (2 × m, CH₂, dppm), 5.44 (s, 5H, Ni-Cp) 6.95–8.07 (m, 40H, Ph). ¹³C NMR (C₆D₆): δ 10.52 (s, C₅Me₅), 28.82–29.60 (m, dppe), 42.29 (m, dppm), 51.50, 91.85, 92.33, 93.27, 107.50, 151.78 (6 × s, C), 90.26 (s, Cp), 94.50 (s, C₅Me₅), 126.99–138.08 (m, Ph), 203.57 (m, Co–CO). ³¹P NMR (C₆D₆): δ 23.6 (s, 2P, Co₃-dppm), 80.3 (s, 2P, Ru-dppe). ES-MS (positive ion mode, MeOH–NaOMe, *m/z*): 1479, [M + Na]⁺; 1456, M⁺.

(g) **With Co₂(CO)₈**. To a mixture of **1** (40 mg, 0.027 mmol) and Co₂(CO)₈ (27 mg, 0.081 mmol) was added thf (10 mL), and the solution was stirred for 20 min. Hexane (30 mL) was then added, and the solution was loaded onto a silica column and eluted with acetone–hexane (1:4). The first fraction contained unreacted Co₂(CO)₈. The second fraction contained the bis-Co₂(CO)₆ adduct {Cp*(dppe)Ru}{C≡CC₂[Co₂(CO)₆]C₂[Co₂(CO)₆]-μ₃-C{Co₃(μ-dppm)(CO)₇} (**11**) (46 mg, 93%) as a dark brown-green solid. *M* = 2048. IR (CH₂Cl₂, cm⁻¹): ν(CO) 2077w, 2055s, 2045m, 2009s, 1991 (sh), 1962 (sh). ¹H NMR (C₆D₆): δ 1.64 (s, 15H, Cp*), 2.14, 2.85 (2 × m, 2 × 2H, CH₂ of dppe), 3.12, 4.41 (2 × 1H, CH₂ of dppm), 6.68–8.15 (m, 55H, Ph). ¹³C NMR (C₆D₆): δ 10.63 (C₅Me₅), 94.65 (s, C₅Me₅), 126.0–135.0 (m, Ph). ³¹P NMR (C₆D₆): δ 33.8 [br d, J(PP) = 24 Hz, 2P], Co₃-dppm], 81.0 (s, 2P, Ru-dppe). ES-MS (positive ion mode, MeOH–NaOMe, *m/z*): 2071, [M + Na]⁺. The complex reverts to **1** if left on silica, on alumina, or in solution in air for more than a day.

Structure Determinations. Full spheres of CCD area-detector diffraction data were measured. *N*_{tot} reflections were merged to *N* unique (*R*_{int} cited) after “empirical”/multiscan absorption correction (proprietary software), *N*_o with *F* > 4σ(*F*) considered “observed”, with all data being used in the full matrix least-squares refinements on *F*². All data were measured using monochromatic Mo Kα radiation, λ = 0.71073 Å. Anisotropic displacement parameter forms were refined for the non-hydrogen atoms, (*x*, *y*, *z*, *U*_{iso})_H being included, constrained at estimates. Residuals *R*, *R*_w on |*F*²| are quoted [weights: (σ₂(*F*²) + *n_w**F*²)⁻¹]. Neutral atom complex scattering factors were used; computation used the XTAL 3.7⁶⁸ or SHELXL 97⁶⁹ program systems. Pertinent results are given in the figures (which show non-hydrogen atoms with 50% probability amplitude displacement ellipsoids and hydrogen atoms with arbitrary radii of 0.1 Å) and in Tables 2 and 4.

Variata. 1•2CHCl₃. One of the two solvent molecules was modeled as rotationally disordered about the C–H bond, site occupancies of the two sets of Cl₃ components each being set at 0.5 after trial refinement.

2. Phenyl ring 42 was modeled as disordered over two sets of sites, occupancies set at 0.5 after trial refinement.

7•1.25C₄H₈O. Diffraction data were very weak, supporting meaningful anisotropic displacement parameter refinement only for Ru, Co, and P. One of the thf solvent molecules, disposed on a crystallographic 2-axis, was assigned site occupancy 0.5 after trial refinement; geometries of both thf components were constrained.

8•2C₆H₆. Phenyl rings 51, 52, 61, and 62 and solvate benzene 30 were modeled as partly or fully disordered over two sets of sites, occupancies set at 0.5 after trial refinement.

8•CH₂Cl₂. This determination was carried out using a synchrotron (Sector 15 of the Advanced Photon Source at the Argonne National Laboratory, Argonne, IL). Full spheres of diffraction data were measured at ca. 103 K with synchrotron radiation, λ = 0.48595 Å.

10•0.32C₆H₁₄. The (centrosymmetric) solvent residues were modeled in terms of C₆H₁₄, site occupancies refining to 0.650(18).

Full details of the structure determinations (except structure factors) have been deposited with the Cambridge Crystallographic Data Centre as CCDC 617992–617997 and 637521. Copies of this information may be obtained free of charge from The Director, CCDC, 12 Union Road, Cambridge CB2 1EZ, UK (fax: + 44 1223 336 033; e-mail: deposit@ccdc.cam.ac.uk or www: http://www.ccdc.cam.ac.uk).

(68) Hall, S. R., du Boulay, D. J., Olthof-Hazekamp, R., Eds. *The XTAL 3.7 System*; University of Western Australia, 2000.

(69) Sheldrick, G. M. *SHELXL-97, Program for Crystal Structure Determination*, Universität Göttingen: Göttingen, 1997.

Acknowledgment. We thank Dr. Maryka Gaudio for assistance with the synthesis of compound Ru{(C≡C)₃SiMe₃}(dppe)Cp* and Professor Brian Nicholson (University of Waikato, Hamilton, New Zealand) for providing the mass spectra. We gratefully acknowledge support of this work by the ARC and by Johnson Matthey plc, Reading, with a generous loan of RuCl₃·*n*H₂O. Use of the ChemMatCARS Sector 15 at the Advanced Photon Source was supported by the Australian Synchrotron Research Program, which is funded by the Commonwealth of Australia under the Major National Research Facilities Program. ChemMat-

CARS Sector 15 is also supported by the National Science Foundation/Department of Energy under Grant Nos. CHE95-22232 and CHE0087817 and by the Illinois Board of Higher Education. The Advanced Photon Source is supported by the U.S. Department of Energy, Basic Energy Sciences, Office of Science, under Contract No. W-31-109-Eng-38.

Supporting Information Available: This material is available free of charge via the Internet at <http://pubs.acs.org>.

OM7010968